GJBX-15(77)

PROVENANCE OF RADIOACTIVE PLACERS, BIG MEADOW AREA VALLEY AND BOISE COUNTIES, IDAHO

BENDIX FIELD ENGINEERING CORPORATION
Grand Junction Operations
Grand Junction, Colorado 81501

February 1977

PREPARED FOR THE U.S. ENERGY RESEARCH AND DEVELOPMENT ADMINISTRATION
GRAND JUNCTION OFFICE, UNDER CONTRACT NO. E(05-1)-1664

GJBX- 15(77)

PROVENANCE OF RADIOACTIVE PLACERS, BIG MEADOW AREA, VALLEY AND BOISE COUNTIES. IDAHO

Dale Truesdell, Richard Wegrzyn, and
Michael Dixon

BENDIX FIELD ENGINEERING CORPORATION
Grand Junction Operations
Grand Junction, Colorado 81501

April 1977

PREPARED FOR THE U.S. ENERGY RESEARCH AND DEVELOPMENT ADMINISTRATION
GRAND JUNCTION OFFICE
UNDER CONTRACT NO. E(05-1)-1664

CONTENTS

ILLUSTRATIONS

SUMMARY

For many years, radioactive black-sand placers have been known to be present in the Bear Valley area of west-central Idaho. The largest of these is in Big Meadow, near the head of Bear Valley Creek. Presence of these placers suggests that low-grade uranium deposits might occur in rocks of the Idaho Batholith, adjacent to Bear Valley. This study was undertaken to locate the provenance of the radioactive minerals and to identify problems that need to be solved before undertaking further investigations.

The principal radioactive minerals in these placers are monazite and euxenite. Other minerals include columbite, samarskite, fergusonite, xenotime, zircon, allanite, sphene, and brannerite. Only brannerite is a uranium mineral; the others contain uranium as an impurity in crystal lattices. All are probably accessory minerals in the plutonic rocks.

Radiometric determinations of the concentration of uranium in stream sediments strongly indicate that the radioactive materials originate in an area drained by Casner and Howard Creeks, which are eastern tributaries to Bear Valley Creek. Previous results by other workers, based on mineralogical studies of stream sediments, support this conclusion. In addition, equivalent uranium levels in bedrock are highest on the divide between Casner and Howard Creeks, which further indicates that this is the probable source for the radioactive placers. However, this area is not known to contain low-grade uranium occurrences.

Euxenite, brannerite, columbite-tantalite, samarskite, and allanite are the principal radioactive minerals that were identified in rock samples. These minerals were found in granite pegmatites, granites, and quartz monzonites. Appreciably higher equivalent uranium concentrations were also found within these rock types.

The major problem encountered in this study was the difficulty in mapping bedrock because of extensive soil and glacial mantle. A partial solution to this problem might be the application of radon emanometry so that radiometric measurements would not be limited to the sparse bedrock samples.

INTRODUCTION

This report presents the results of an investigation to determine the presence of low-grade uranium occurrences in rocks of the Idaho Batholith near radioactive placers in the Big Meadow part of Bear Valley, Boise, and Valley Counties, Idaho. The project began July 1, 1975, and was concluded March 30, 1976. The study was conducted for the Grand Junction Office of the U.S. Energy Research and Development Administration (ERDA).

PROBLEM

Radioactive black-sand placers in Big Meadow have been known for over two decades. Porter Brothers Corporation dredged about 200,000 tons of the placers in the period 1955 to 1960 but ceased operations because of difficulty in marketing rare-earth elements. The firm operated a heavy-minerals separation mill at Lowman, Idaho, to recover columbite-euxenite and monazite concentrates, plus other potentially valuable by-products, such as magnetite, ilmenite, zircon, and garnet. Porter Brothers held a contract with the AEC for the sale of uranium oxide extracted from the concentrates by the Mallinckrodt Chemical Works at Hematite, Missouri; and some by-product magnetite and ilmenite were shipped to the AEC in Las Vegas, Nevada, for steming material.

The presence of placers in Big Meadow indicates that a source of uranium-bearing radioactive minerals may be in the bedrock near Bear Valley, as suggested by Mackin and Schmidt (1953) from results of a mineralogic and petrologic study of placer and colluvial materials. According to Armstrong (1974) a more precise identification of such a source might therefore lead to discovery of low-grade uranium occurrences.

OBJECTIVE AND SCOPE

The principal objective of this study was to locate and identify, by means of a radiometric survey, the provenance for the radioactive placers found in the Big Meadow area. In addition, problems that require resolution prior to undertaking larger studies of a similar nature were to be isolated and identified. The investigation included a literature survey of previous work in the area, an examination of the radioactive placers to determine the minerals present, and radiometric analyses of bedrock and stream-sediment samples.

The area investigated (Figs. 1-3) encompasses approximately 12 sq mi. It is bounded on the west by Bear Valley Creek, on the south by the Valley County line, on the east by Red Mountain and Cache Creek, and on the north by Mace Meadows.

PREVIOUS WORK

Studies of the radioactive placers were conducted for the AEC by Kline and others (1953) and by Mackin and Schmidt (1953, 1956). Additional

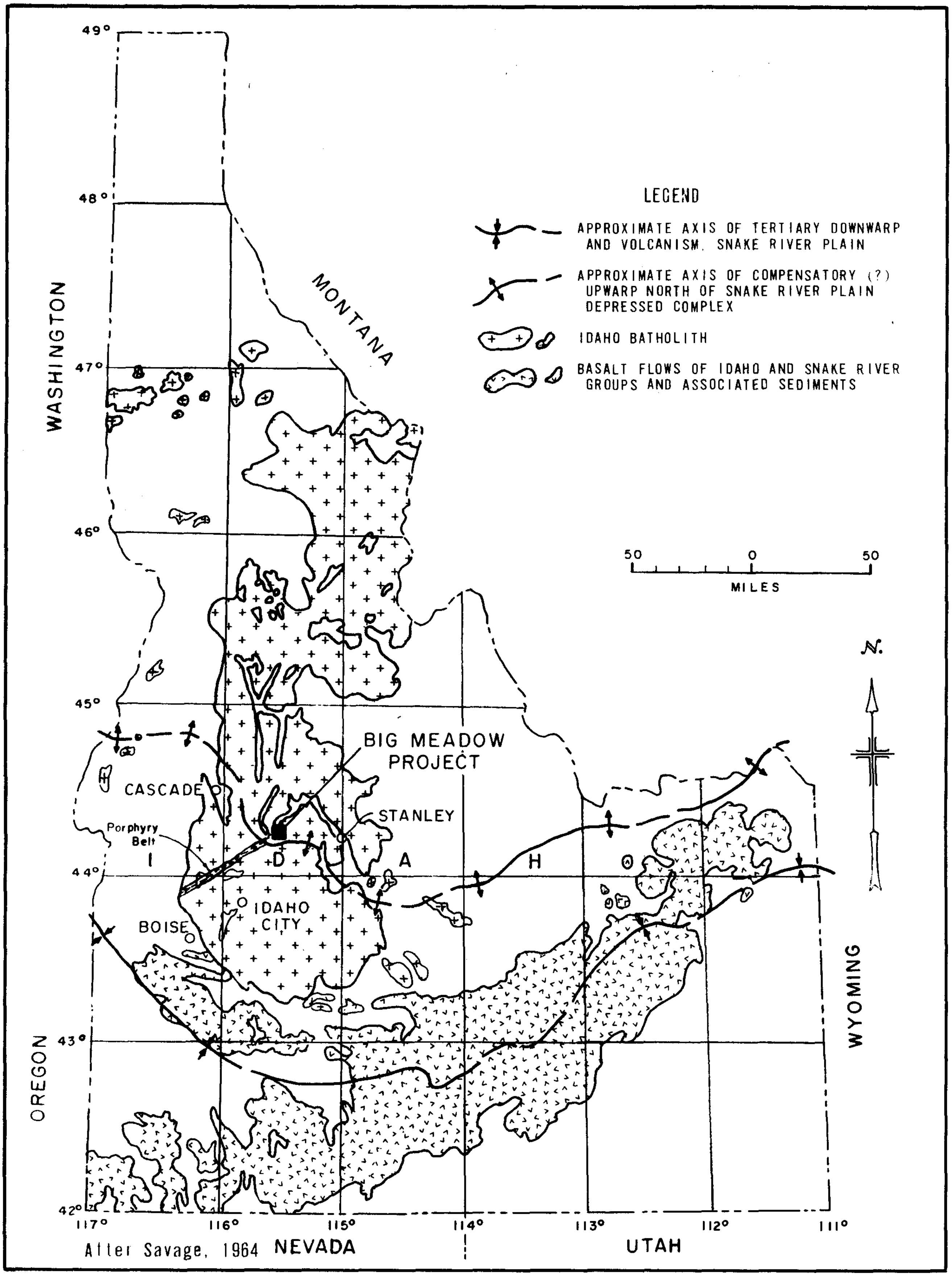

Figure 1. Geologic setting of Big Meadow placers.

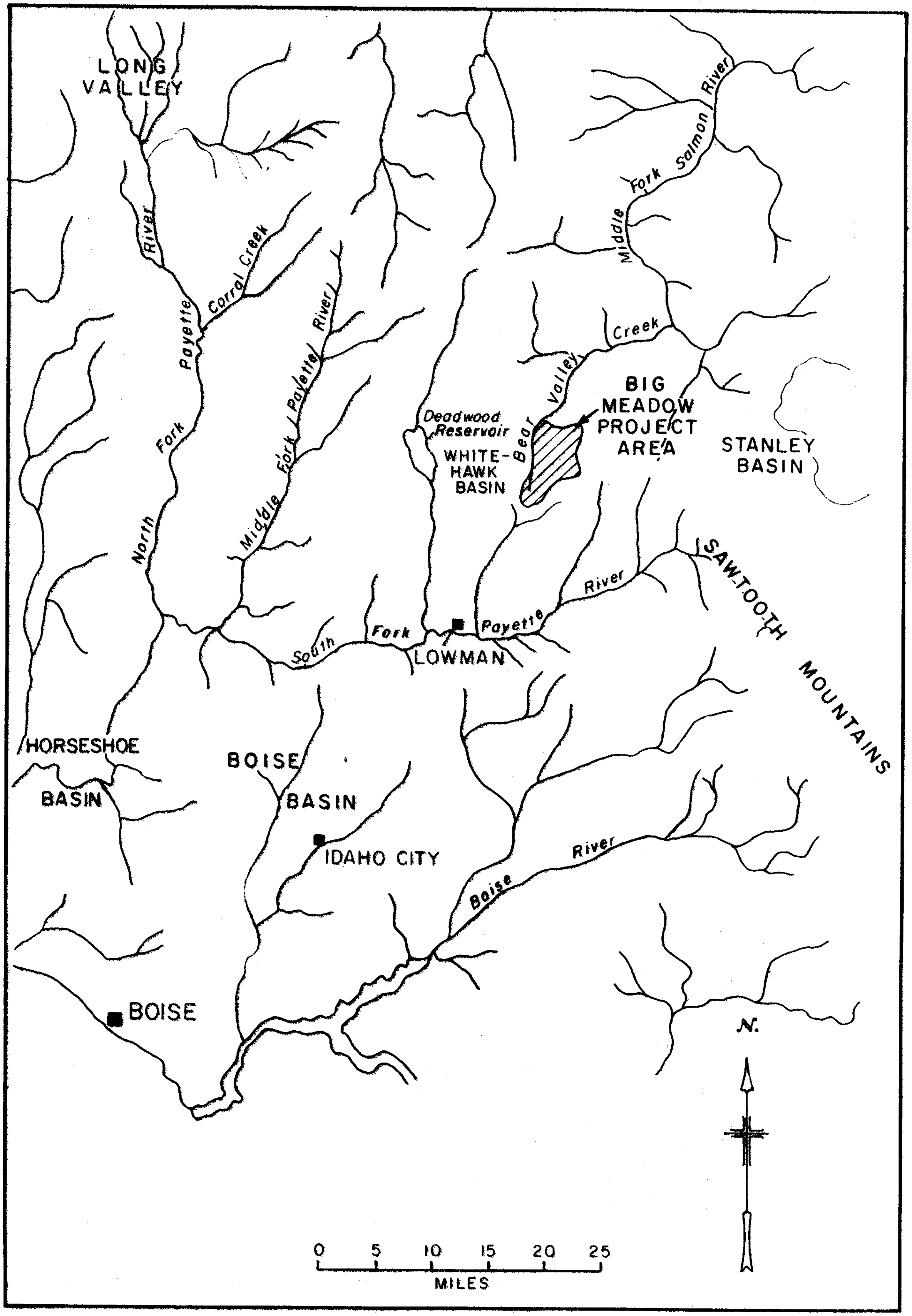

Figure 2. Regional stream drainage of west-central Idaho.

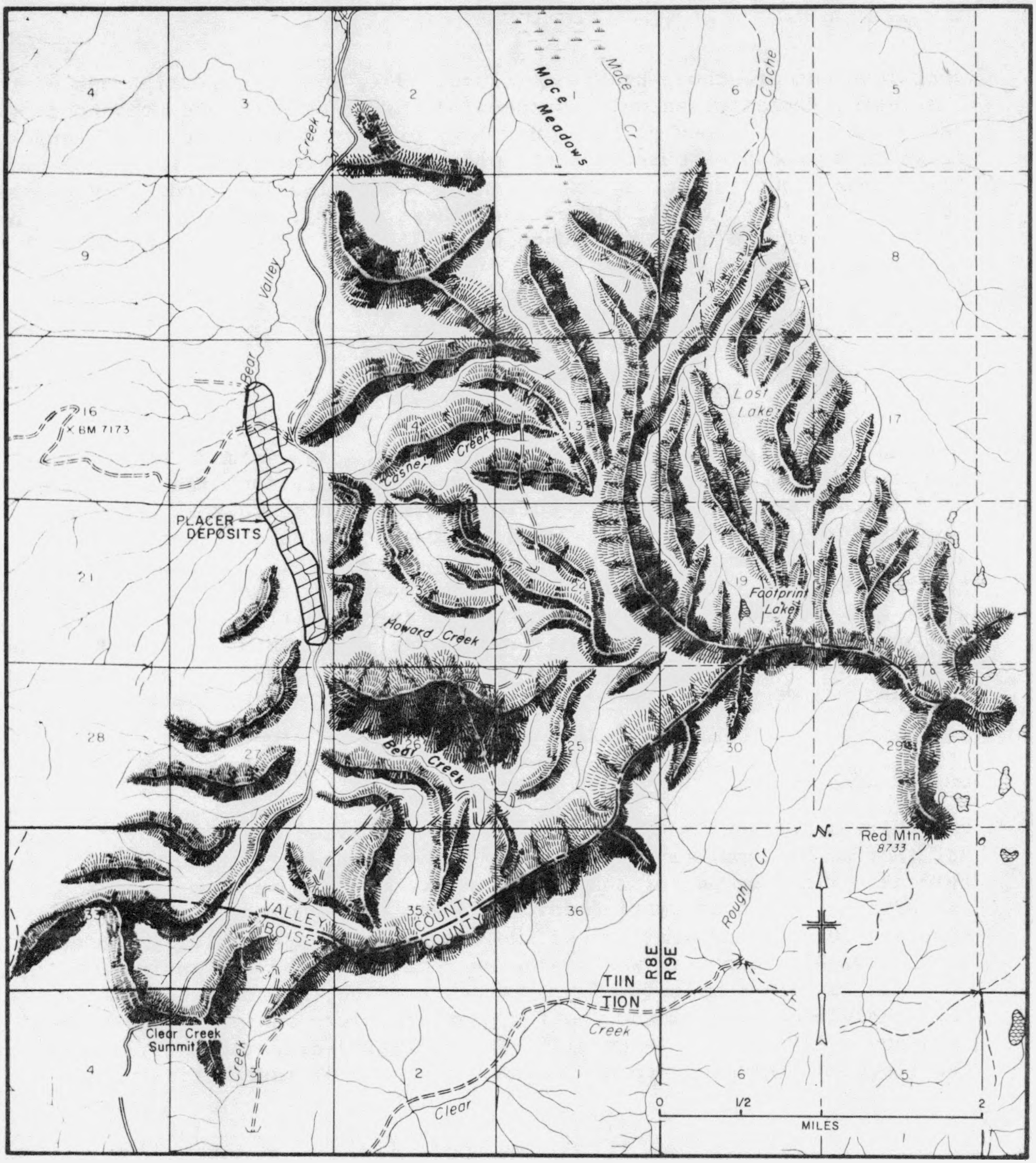

Figure 3. Physiographic sketch map of project area.

contributions are those by Savage (1960, 1961, 1964). Descriptions of the black-sand deposits, as well as speculations on origin, are presented by these authors; a study of the mineralogy of stream sediments and bedrock, in which a probable source for the placers was determined, is an especially significant contribution by Mackin and Schmidt (1953). Studies by Anderson (1942, 1947, 1948, 1952), Larsen and others (1958), and Schmidt (1964) provide useful information about the Idaho Batholith and the rock types found in central Idaho.

PROCEDURES

FIELD

An initial reconnaissance of the project area was made to ascertain the extent of bedrock exposure in order that a suitable sampling program could be devised. Rock samples were collected from sparse bedrock outcrops (Fig. 4) for petrographic examination and elemental analysis; effort was made to sample each rock type distinguished in the field. In addition, stream-sediment samples (Fig. 4) were taken from eastern tributaries of Bear Valley Creek and from Cache Creek tributaries in the Footprint Lake - Lost Lake area on the basis of indications from Mackin and Schmidt (1953) that a probable provenance for radioactive placers was in these drainage areas. Radioactivity was measured at each sample site with a hand-held scintillometer.

LABORATORY

Stream-sediment and rock samples were analyzed for equivalent uranium and thorium by gamma-ray spectroscopy (Apps. A and C). Bedrock lithologies were determined by petrographic examination of thin sections (Apps. C and D). In addition, the nonmagnetic heavy-mineral fractions of the fine-grained separate (0.6 mm and smaller) of the stream-sediment samples was assayed for U_3O_8 (App. B). Emphasis was placed on recognition of the radioactive placer minerals in rock samples. Eight bedrock samples, selected because of their high equivalent uranium and thorium contents, were analyzed by semiquantitative emission spectroscopy, x-ray diffraction, energy-dispersive x-ray fluorescence, and electron microscopy to determine the source of radioactivity.

GEOLOGY

Big Meadow is near the center of the Idaho Batholith (Fig. 1), which is of early Late Cretaceous age (Larsen and others, 1958, p. 51). In the project area, the batholith is composed mainly of quartz monzonite, granite, and quartz diorite. According to Anderson (1952, p. 257), these rocks were emplaced under deep-seated conditions and are characteristic of the inner facies of the batholith. Pegmatite and aplite dikes, which formed during late stages of consolidation, fill fractures that are principally oriented northwestward. Diorite dikes and stocks were formed in early Tertiary time and are spatially

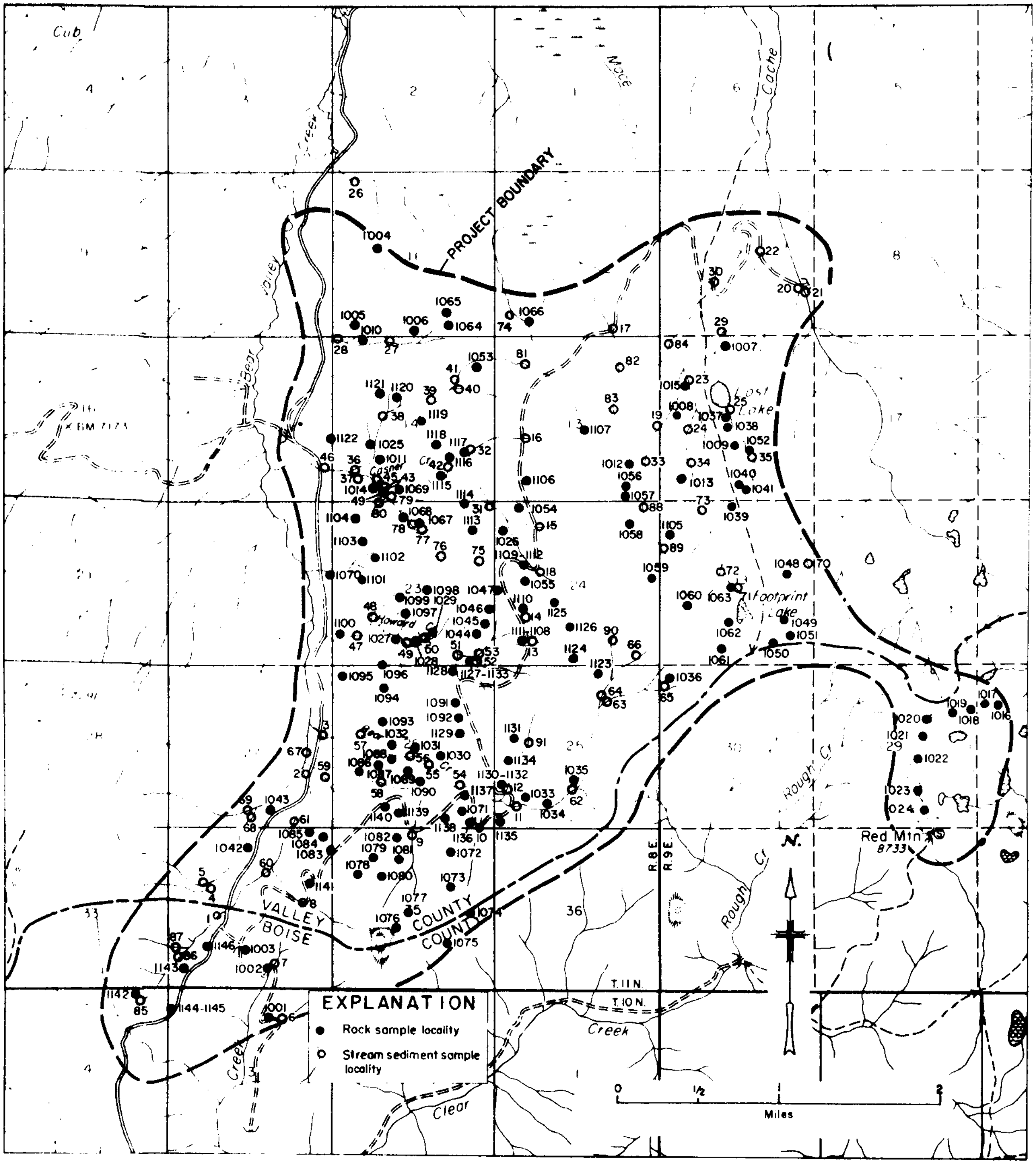

Figure 4. Map showing localities sampled and sample identification numbers.

associated with northeastward lines of weakness. A prominent belt (Fig. 1) of middle Tertiary porphyry intrusions, recognized in the Horseshoe and Boise Basins areas (Fig. 2), extends in a northeastward direction just south of the project area (Anderson, 1947).

The present drainage pattern in central Idaho (Fig. 2) was established in Miocene time (Anderson, 1947) when uplift, collapse, and faulting occurred. The axis of uplift (Fig. 1) passes immediately south of Big Meadow. Alterations in erosion patterns resulted in stream piracy, and a "one-sided" drainage pattern was formed in which trunk streams drained to the west and their tributaries drained from the north (Fig. 2). Block faulting and intermittent uplift at the close of Pliocene time led to the present regional elevation and stream dissection.

BIG MEADOW PLACERS

DESCRIPTION

Major radioactive placer deposits are found in the alluvium that composes the floor of Big Meadow, a large parklike area in the upper reaches of Bear Valley Creek (Fig. 3). The locations of the placers are easily recognizable by the numerous dredge tailings evident in the area. As much as 100 ft of alluvium, which contains lenses of radioactive black sands, were deposited in a detritus trap that was produced by the blockage of Bear Valley Creek by an Illinoian glacier (Mackin and Schmidt, 1953). Drilling and sampling investigations by the U.S. Bureau of Mines for the AEC (Kline and others, 1953) indicate that the richest placers are near the mouths of Casner and Howard Creeks, both of which are tributaries flowing into Bear Valley Creek from the east (Fig. 3).

Alluvium found in Big Meadow consists predominantly of arkosic sand and gravel containing a heavy-mineral fraction that includes several radioactive minerals. The principal radioactive placer minerals are monazite and euxenite (Schmidt, 1964, p. 3). Minor minerals identified in this study, and also by Kline and others (1953, p. 5-6), include columbite, samarskite, fergusonite, xenotime, zircon, allanite, and sphene. Analyses of heavy-mineral separates also demonstrate the presence of brannerite, which is the only true uranium mineral found in the placers. Brannerite and samarskite were found to be closely associated with one another in dull black grains, but the precise nature of their association could not be determined. Samarskite was also found as distinct inclusions in grains of euxenite.

PROVENANCE

Past studies to determine the origin of the Big Meadow placers have been based principally upon analyses of the minerals composing stream sediments and bedrock in and adjacent to Bear Valley, and there appears to be little or no disagreement among previous workers that the radioactive minerals came from a source to the east of Bear Valley. Results of radiometric analyses of stream sediment and bedrock examined during this project confirm the previous findings and further delineate a probable source area.

RESULTS OF STREAM-SEDIMENT ANALYSES

Stream sediments that contain the highest equivalent uranium concentrations are found in the valleys of Howard and Casner Creeks (Fig. 5). Uranium in the heavy-mineral fraction shows an areal distribution (Fig. 6) very similar to that determined by radiometric analyses performed on gross sediment samples; this indicates, therefore, that radioactivity is coming principally from the heavy minerals. Drilling and sampling of the Big Meadow placers by the U.S. Bureau of Mines for the AEC (Kline and others, 1953) demonstrated that the richest placers were derived from Casner Creek (Howard Creek sediments were not drilled and sampled). Mackin and Schmidt (1953, p. 10) found that residual soil in the Casner and Howard Creeks drainage basins contained as much as 1 lb of radioactive black materials per cubic yard; stream-bed materials contained as much as 4 lbs per cubic yard, whereas materials from other areas contained much less. Thus, both mineralogic and radiometric analyses provide results pointing to bedrock drained by Casner and Howard Creeks as a source for the radioactive placers.

RESULTS OF BEDROCK ANALYSES

Despite attempts by previous workers to trace the placers to a particular bedrock source, no single source has been isolated. In their initial study, Mackin and Schmidt (1953, p. 4) concluded that monazite was an accessory mineral in granitic rocks of the Idaho Batholith, whereas the other radioactive black sands came from pegmatite dikes. They later (1956, p. 588) revised their interpretation to agree with that of Kline and others (1953, p. 9), who believed that all the placer minerals were derived from both the granites and the associated pegmatites. Savage (1960, p. 795; 1961, p. 61) suggested that the placers came from pegmatite and aplite dikes on the west and northwest flanks of Red Mountain (Fig. 3).

In the present study, 21 lithologies, based on both field criteria and thin-section analyses and using the rock classification of Travis (1955), were identified from examination of bedrock samples. These include quartz pegmatite, aplite, granodiorite pegmatite, quartz diorite pegmatite, pneumatolytic quartz diorite pegmatite, quartz monzonite pegmatite, granite pegmatite, quartz diorite, altered/deformed quartz diorite, granodiorite, quartz monzonite, granite, hornblende andesite porphyry, andesite porphyry, hornblende diorite porphyry, diorite porphyry, dacite porphyry, quartz latite porphyry, hornblende andesite, andesite, and amphibolite (App. D). Radiometric determinations of uranium in each bedrock sample indicate that granite pegmatites and quartz monzonites contain the highest average uranium concentrations (Table 1; Fig. 7).

Polymorphism, metamict nature, and similarity of structures made visual identification of uranium- and thorium-bearing multiple-oxide minerals difficult.

TABLE 1. EQUIVALENT URANIUM AND THORIUM CONTENTS OF THE ROCK TYPES PRESENT IN THE BIG MEADOW AREA.

Rock type	Number	eU (ppm) Range	eU (ppm) Average	eTh (ppm) Range	eTh (ppm) Average
Quartz pegmatites	5	0.0- 2.8	0.7	0.0-14.0	3.5
Aplites	5	1.8- 4.8	2.8	3.3- 9.1	6.1
Granodiorite pegmatites	5	1.6- 3.9	3.8	2.3- 9.0	5.3
Quartz diorite pegmatites	18	0.1- 9.6	4.1	2.8-16.2	6.9
"Pneumatolytic" quartz diorite pegmatite	1	- -	1.2	- -	3.4
Quartz monzonite pegmatites	13	0.9-18.1	4.5	1.1-15.1	6.4
Granite pegmatites	29	0.0-37.0	8.3	1.1-16.7	7.7
Quartz diorites	9	1.1- 3.0	2.0	6.9-25.3	11.4
Altered/deformed quartz diorites	2	1.2- 7.1	4.1	9.7-11.2	10.4
Granodiorites	19	0.6-12.4	2.1	7.4-16.9	12.8
Quartz monzonites	41	0.2-93.1	6.4	2.5-32.5	12.3
Granites	26	1.1-21.7	3.0	2.0-22.3	10.6
Hornblende andesite porphyries	5	1.5- 2.8	2.1	6.7-13.8	10.7
Andesite porphyries	31	1.6-18.1	3.3	7.1-16.7	12.3
Hornblende diorite porphyry	1	- -	1.8	- -	10.6
Diorite porphyries	5	1.6- 2.9	2.1	11.6-18.2	14.9
Dacite porphyries	3	2.4- 2.9	2.6	11.7-15.9	13.6
Quartz latite porphyries	3	2.6- 5.2	4.2	13.8-24.3	20.1
Hornblende	4	0.7- 1.7	1.3	5.1- 6.9	6.2
Andesite	1	- -	1.2	- -	8.9
Amphibolite xenoliths	2	3.6- 3.9	3.7	5.4- 7.2	6.3

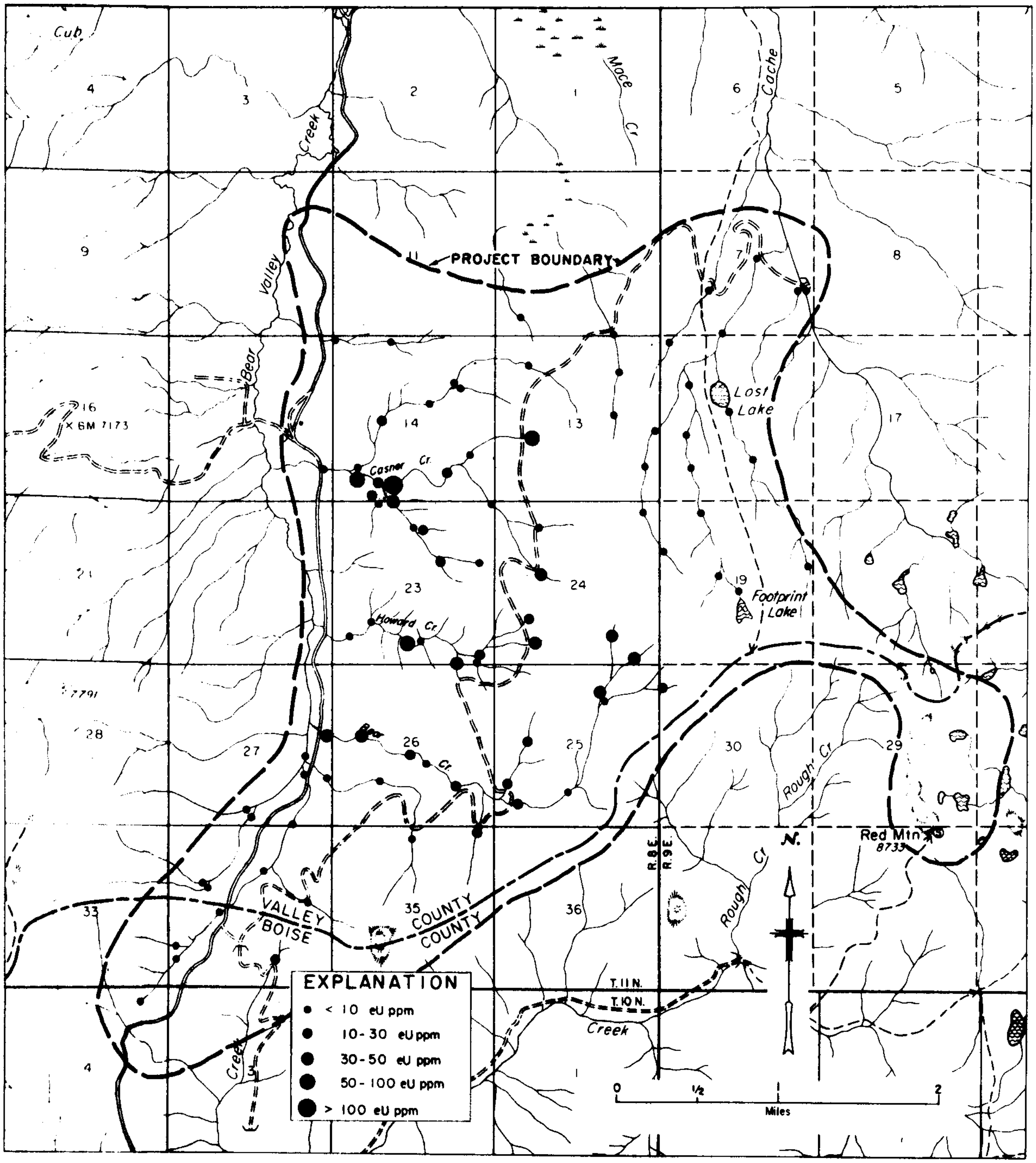

Figure 5. Uranium in stream-sediment samples.

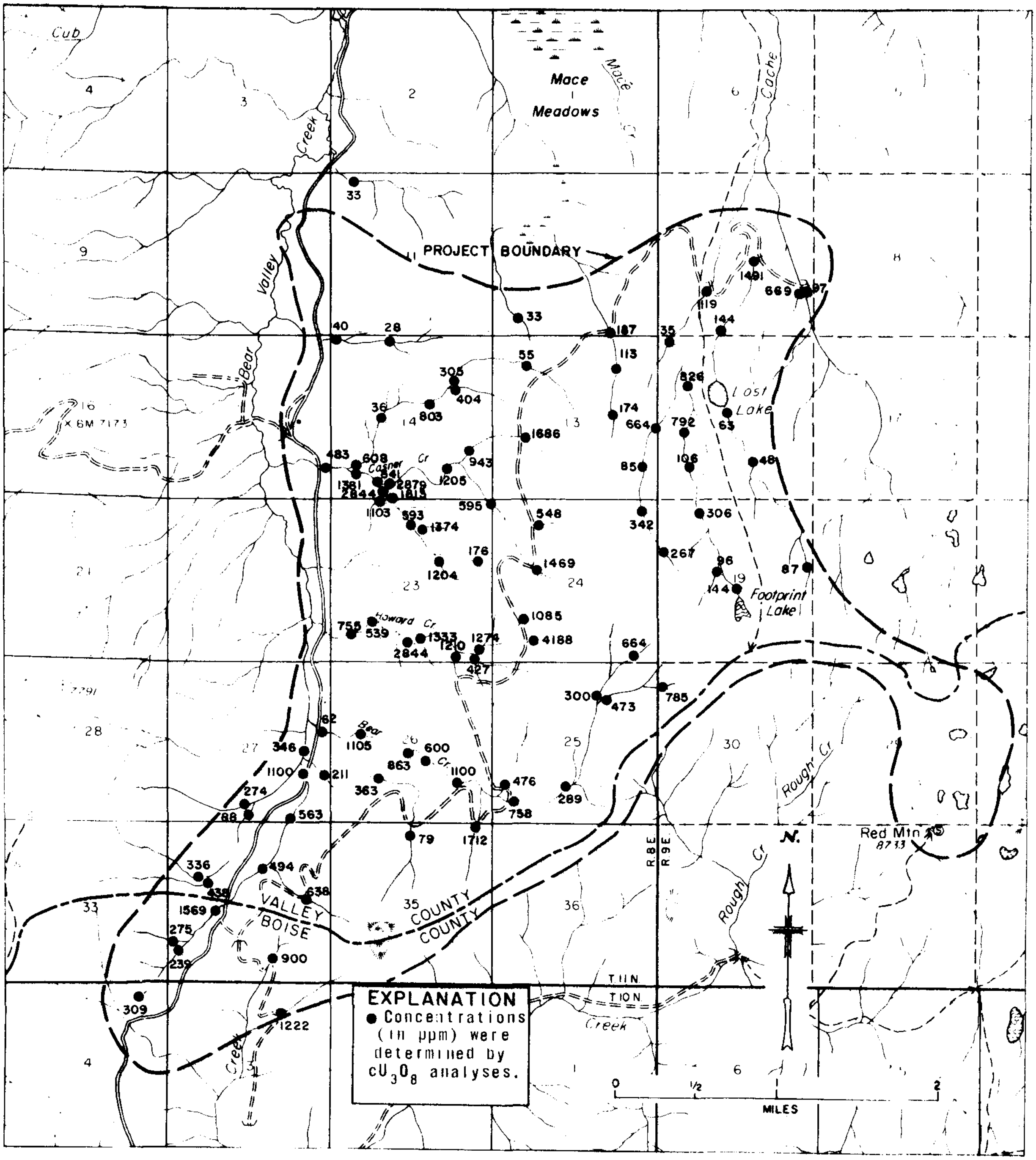

Figure 6. Uranium in nonmagnetic heavy-mineral fraction of stream-sediment samples.

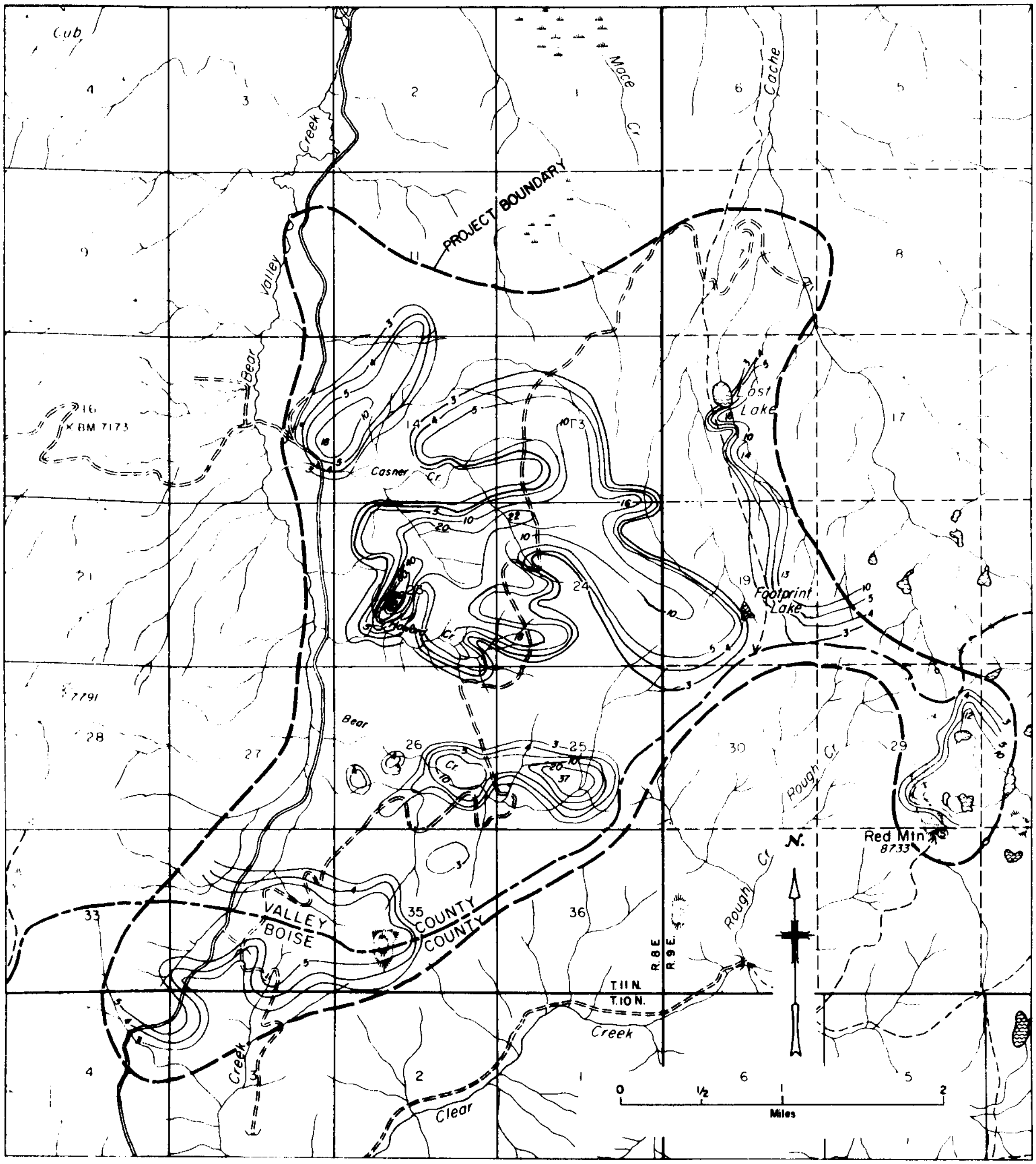

Figure 7. Radiometric uranium concentrations in bedrock.

In an effort to determine the presence of these minerals, the six samples with the highest radiometric eU contents were chosen for more intense study. The heavy-mineral fractions of these six samples were analyzed by semiquantitative emission spectrographic analysis to help identify these minerals (Table 2). Scanning electron microscopy and energy dispersive x-ray analysis coupled with x-ray diffraction were the analytical tools employed.

Euxenite [(Y, Ca, Ce, U, Th) $(Nb, Ta, Ti)_2O_6$] was found in samples 1054-1 (granite pegmatite), 1113-1 (granite pegmatite), and 1122-1 (granite pegmatite). Brannerite [$(U, Ca, Fe, Y, Th)_3Ti_5O_{16}$] was found in sample 1035-1 (granite pegmatite). Samarskite [(Y, Er, Ce, U, Ca, Fe, Pb, Th) $(Nb, Ta, Ti, Sn)_2O_6$] and columbite-tantalite [(Fe, Mn) $(Nb, Ta)_2O_6$] were found in samples 1067-2 (granite) and 1099-1 (quartz monzonite). In addition, slightly radioactive allanite was found in these and other samples.

Radiometric analysis of the samples indicates that an area drained by Casner and Howard Creeks contains the most radioactive material (Fig. 7) and that this area (sec. 23, T. 11 N., R. 8 E.) is the most likely source of the minute grains of radioactive accessory minerals composing the Big Meadow placers.

CONCLUSIONS

On the basis of the results of this study and previous investigations by others, the following conclusions were reached:

1. Uranium in the Big Meadow placers occurs principally as impurities in the crystal lattices of accessory minerals, such as euxenite, samarskite, allanite, and monazite, that were derived from the "granitic" bedrock of the Idaho Batholith. The uranium mineral brannerite, which is found both in bedrock and placers, is too rare to have produced all the observed radioactivity.

2. The principal radioactive minerals are associated with several different rock types.

3. Radiometric determinations of uranium in stream-sediment and bedrock samples strongly suggest that the provenance of the radioactive placers is an area drained by Casner and Howard Creeks.

4. Radiometric determinations suggest that the two principal sources of the detrital uranium were granite pegmatites and quartz monzonites.

5. Results of this and previous investigations are insufficient to demonstrate that low-grade uranium occurrences are to be found in the bedrock around Big Meadow.

6. Stream-sediment sampling is a recommended technique for general use in exploring the Idaho Batholith. This procedure should, however, be accompanied by analyses of both mantle and bedrock material in order to better delineate source areas and possible low-grade uranium deposits.

TABLE 2. PARTIAL SEMIQUANTITATIVE EMISSION-SPECTROGRAPHIC ANALYSES OF HEAVY-MINERAL SEPARATES FROM SELECT BEDROCK SAMPLES.

Element	(% concentration in sample no.) 1035-3	1054-1	1067-2	1099-1	1113-1	1122-1
Ca	3.0000	1.0000	2.0000	1.5000	4.0000	0.5000
Ce	0.0400	0.0100	0.0200	0.0300	0.0300	0.0300
Co	0.0030	0.0020	0.0030	0.0030	0.0080	0.0050
Cr	0.0040	0.0200	0.0050	0.0030	0.0300	0.0500
Cu	0.0030	0.0050	0.0040	0.0030	0.0100	0.0070
Dy	0.0050	0.0040	0.0020	0.0070	0.0090	0.0060
Eu	0.0020	0.0010	0.0010	0.0030	0.0050	0.0010
Gd	0.0080	0.0060	0.0060	0.0070	0.0100	0.0070
Ho	0.0040	0.0050	0.0020	0.0050	0.0040	0.0030
La	0.0100	0.0030	0.0040	0.0050	0.0070	0.0030
Lu	0.0030	0.0030	0.0010	0.0020	0.0050	0.0020
Mn	0.7000	0.2000	0.7000	0.9000	0.9000	0.1000
Mo	0.0020	0.0020	0.0010	0.0020	0.0020	0.0030
Nb	0.4000	0.6000	0.1000	0.1500	0.6000	>1.0000
Ni	0.0050	0.0500	0.0040	0.0020	0.0200	0.0600
P	0.5000	0.1000	0.1500	0.2000	1.0000	0.1000
Pb	0.0080	0.0090	0.0050	0.0050	0.0080	0.0080
Pr	0.0040	0.0050	0.0040	0.0030	0.0030	0.0060
Sc	0.0030	0.0020	0.0060	0.0060	0.0050	0.0020
Sm	0.0040	0.0030	0.0040	0.0040	0.0070	0.0060
Ta	0.0050	0.0050	<0.0200	0.0030	0.0100	0.0300
Th	0.1000	0.0800	0.0800	0.4000	0.4000	0.1500
Ti	>1.0000	>1.0000	>1.0000	>1.0000	>1.0000	>1.0000
U	0.3000	0.2000	0.1500	0.1000	0.5000	0.3000
V	0.0200	0.0300	0.0400	0.0300	0.0200	0.0300
W	0.0500	0.0400	0.0100	0.0200	0.1000	0.1500
Y	0.0700	0.0600	0.0200	0.0700	0.1500	0.0800
Yb	0.0080	0.0090	0.0020	0.0100	0.0200	0.0080
Zn	0.0500	0.0600	0.0600	0.0600	0.0800	0.0600
Zr	0.2500	0.2500	0.2000	0.1500	0.2000	0.0500

7. The major problem encountered in this study was the difficulty of mapping bedrock because of extensive soil and glacial mantle. A partial solution to this problem might be the application of radon emanometry so that radiometric measurements would not be limited to the sparse bedrock samples.

BIBLIOGRAPHY

Anderson, A. L., 1942, Endomorphism of the Idaho Batholith: Geol. Soc. America Bull., v. 53, p. 1099-1126.

_____1947, Geology and ore deposits of Boise Basin, Idaho: U.S. Geol. Survey Bull. 944-C, 319 p.

_____1948, Role of the Idaho Batholith during the Laramide Orogeny: Econ. Geology, v. 43, no. 2, p. 84-99.

_____1952, Multiple emplacement of the Idaho Batholith: Jour. Geology, v. 60, p. 255-265.

Armstrong, F. C., 1974, Uranium resources of the future-"porphyry" uranium deposits, in Formation of uranium ore deposits: Vienna, Austin, Internat. Atomic Energy Agency, p. 625-634.

Kline, M. H., and Carlson, E. J., 1954, Pearsol Creek monazite placer area, Valley County, Idaho: U.S. Bur. Mines RME-3134, issued by U.S. Atomic Energy Comm., Office of Tech. Inf. Services, Oak Ridge, Tenn., 24 p.

Kline, M. H., Carlson, E. J., and Griffith, R. H., 1950, Boise Basin monazite placers, Boise County, Idaho: U.S. Bur. Mines RME-3129, issued by U.S. Atomic Energy Comm., Office of Tech. Inf. Services, Oak Ridge, Tenn., 37 p.

Kline, M. H., Carlson, E. J., Storch, R. H., and Robertson, A. F., 1953, Bear Valley radioactive mineral placers, Valley County, Idaho: U.S. Bur. Mines RME-3130, issued by U.S. Atomic Energy Comm., Office of Tech. Inf. Services, Oak Ridge, Tenn., 23 p.

Kline, M. H., Carlson, E. J., and Horst, H. W., 1955, Corral Creek monazite placer area, Valley County, Idaho: U.S. Bur. Mines RME-3135, issued by U.S. Atomic Energy Comm., Office of Tech. Inf. Services, Oak Ridge, Tenn., 22 p.

Larsen, E. S., Gottfried, D., Jaffe, H. W., and Waring, C. L., 1958, Lead-alpha ages of the Mesozoic batholiths of western North America: U.S. Geol. Survey Bull. 1070-B, p. 35-62.

Mackin, J. H., and Schmidt, D. L., 1953, Reconnaissance geology of placer deposits containing radioactive minerals in the Bear Valley district, Valley County, Idaho: U.S. Geol. Survey TEM 602, issued by U.S. Atomic Energy Comm., Office of Tech. Inf. Services, Oak Ridge, Tenn., 32 p.

_____1956, Uranium and thorium bearing minerals in placer deposits in Idaho, in Vol. 6, Geology of uranium and thorium: Geneva, Switzerland, Internat. Conf. on the Peaceful uses of Atomic Energy, p. 587-592.

Ross, C. P., 1934a, Some lode deposits in the northwestern part of the Boise Basin, Idaho: U.S. Geol. Survey Bull. 846-D, p. 239-277.

BIBLIOGRAPHY (continued)

Rose, C. P., 1934b, Geology and ore deposits of the Casto quadrangle, Idaho: U.S. Geol. Survey Bull. 854, 135 p.

Savage, C. N., 1960, Nature and origin of central Idaho blacksands: Econ. Geology, v. 55, p. 789-796.

_____1961, Economic geology of central Idaho blacksand placers: Idaho Bur. Mines and Geology Bull. 17, 160 p.

_____1964, Preliminary tectonic map of Idaho: Idaho Bur. Mines and Geology.

Schmidt, D. L., 1964, Reconnaissance petrographic cross section of the Idaho Batholith in Adams and Valley Counties, Idaho: U.S. Geol. Survey Bull. 1181-G, p. GI-G50.

Travis, R. B., 1955, Classification of rocks: Golden, Colorado School Mines Quart., v. 50, No. 1, 98 p.

APPENDIX A

GAMMA-RAY SPECTROMETRIC ANALYSES
OF STREAM-SEDIMENTS SAMPLES

APPENDIX A.

GAMMA-RAY SPECTROMETRIC ANALYSES OF STREAM-SEDIMENT SAMPLES

Sample No.	Location	eU ppm	eTh ppm
1	SW¼ sec. 34, T. 11 N., R. 8 E.	3.7	7.2
2	SE¼ sec. 27, T. 11 N., R. 8 E.	6.1	11.1
3	NE¼ sec. 27, T. 11 N., R. 8 E.	35.6	18.4
4	NW¼ sec. 34, T. 11 N., R. 8 E.	1.4	6.0
5	NW¼ sec. 34, T. 11 N., R. 8 E.	2.7	6.1
6	NE¼ sec. 3, T. 11 N., R. 8 E.	2.4	7.4
7	SE¼ sec. 34, T. 11 N., R. 8 E.	10.6	16.9
8	NE¼ sec. 34, T. 11 N., R. 8 E.	5.9	8.9
9	NE¼ sec. 35, T. 11 N., R. 8 E.	2.8	8.1
10	SE¼ sec. 26, T. 11 N., R. 8 E.	15.7	13.9
11	SW¼ sec. 25, T. 11 N., R. 8 E.	10.5	10.0
12	SW¼ sec. 25, T. 11 N., R. 8 E.	20.0	14.5
13	SW¼ sec. 24, T. 11 N., R. 8 E.	32.0	19.8
14	SW¼ sec. 24, T. 11 N., R. 8 E.	10.4	9.0
15	NW¼ sec. 24, T. 11 N., R. 8 E.	5.3	7.5
16	SW¼ sec. 13, T. 11 N., R. 8 E.	51.2	26.4
17	SE¼ sec. 12, T. 11 N., R. 8 E.	2.2	8.1
18	NW¼ sec. 24, T. 11 N., R. 8 E.	48.3	25.1
19	SW¼ sec. 19, T. 11 N., R. 9 E.	6.4	13.5
20	SE¼ sec. 7, T. 11 N., R. 9 E.	2.3	7.4
21	SE¼ sec. 7, T. 11 N., R. 9 E.	1.8	8.0
22	NE¼ sec. 7, T. 11 N., R. 9 E.	2.4	8.6
23	NW¼ sec. 25, T. 11 N., R. 9 E.	1.7	7.3
24	SW¼ sec. 25, T. 11 N., R. 9 E.	1.9	5.8
25	NW¼ sec. 25, T. 11 N., R. 9 E.	2.8	7.9
26	NW¼ sec. 11, T. 11 N., R. 8 E.	1.6	12.9
27	NW¼ sec. 14, T. 11 N., R. 8 E.	1.1	4.5
28	NW¼ sec. 14, T. 11 N., R. 8 E.	1.8	6.4
29	SW¼ sec. 7, T. 11 N., R. 9 E.	2.5	9.1
30	SW¼ sec. 7, T. 11 N., R. 9 E.	3.4	9.7
31	NE¼ sec. 23, T. 11 N., R. 8 E.	7.6	11.9
32	SE¼ sec. 14, T. 11 N., R. 8 E.	2.9	4.2
33	SE¼ sec. 13, T. 11 N., R. 8 E.	1.4	5.9
34	SW¼ sec. 18, T. 11 N., R. 9 E.	1.0	4.5
35	SE¼ sec. 19, T. 11 N., R. 9 E.	0.5	4.0
36	SW¼ sec. 14, T. 11 N., R. 8 E.	1.2	5.5
37	SW¼ sec. 14, T. 11 N., R. 8 E.	78.8	56.3
38	NW¼ sec. 14, T. 11 N., R. 8 E.	17.5	19.5
39	NE¼ sec. 14, T. 11 N., R. 8 E.	7.0	13.0
40	NE¼ sec. 14, T. 11 N., R. 8 E.	2.1	5.3
41	NE¼ sec. 14, T. 11 N., R. 8 E.	4.7	14.4
42	SE¼ sec. 14, T. 11 N., R. 8 E.	70.1	17.8
43	SW¼ sec. 14, T. 11 N., R. 8 E.	123.7	59.3
44	SW¼ sec. 14, T. 11 N., R. 8 E.	13.7	17.7

Sample No.	Location	eU ppm	eTh ppm
45	SW¼ sec. 14, T. 11 N., R. 8 E.	19.2	17.4
46	SE¼ sec. 15, T. 11 N., R. 8 E.	6.4	10.5
47	SW¼ sec. 23, T. 11 N., R. 8 E.	3.8	10.5
48	SW¼ sec. 23, T. 11 N., R. 8 E.	4.2	8.0
49	SW¼ sec. 23, T. 11 N., R. 8 E.	67.5	39.7
50	SE¼ sec. 23, T. 11 N., R. 8 E.	1.5	3.4
51	SE¼ sec. 23, T. 11 N., R. 8 E.	44.1	24.0
52	SE¼ sec. 23, T. 11 N., R. 8 E.	4.6	8.6
53	SE¼ sec. 23, T. 11 N., R. 8 E.	27.6	22.3
54	SE¼ sec. 26, T. 11 N., R. 8 E.	25.1	23.7
55	SE¼ sec. 26, T. 11 N., R. 8 E.	3.9	7.8
56	SW¼ sec. 26, T. 11 N., R. 8 E.	20.9	19.8
57	NW¼ sec. 27, T. 11 N., R. 8 E.	41.8	32.3
58	SW¼ sec. 26, T. 11 N., R. 8 E.	2.5	7.4
59	SE¼ sec. 27, T. 11 N., R. 8 E.	1.1	4.8
60	NE¼ sec. 34, T. 11 N., R. 8 E.	1.3	5.9
61	SE¼ sec. 27, T. 11 N., R. 8 E.	4.7	11.9
62	SW¼ sec. 25, T. 11 N., R. 8 E.	2.8	8.5
63	NW¼ sec. 25, T. 11 N., R. 8 E.	3.5	2.2
64	NE¼ sec. 25, T. 11 N., R. 8 E.	39.1	25.1
65	NW¼ sec. 30, T. 11 N., R. 9 E.	11.1	11.3
66	SE¼ sec. 24, T. 11 N., R. 8 E.	33.5	27.7
67	SE¼ sec. 27, T. 11 N., R. 8 E.	3.5	11.2
68	SW¼ sec. 27, T. 11 N., R. 8 E.	0.9	4.0
69	SW¼ sec. 27, T. 11 N., R. 8 E.	2.2	4.9
70	NE¼ sec. 19, T. 11 N., R. 9 E.	1.7	8.3
71	SE¼ sec. 19, T. 11 N., R. 9 E.	3.4	10.9
72	NW¼ sec. 19, T. 11 N., R. 9 E.	0.7	3.4
73	NW¼ sec. 19, T. 11 N., R. 9 E.	1.3	6.0
74	SW¼ sec. 6, T. 11 N., R. 8 E.	0.8	3.9
75	NE¼ sec. 23, T. 11 N., R. 8 E.	4.4	8.2
76	NE¼ sec. 23, T. 11 N., R. 8 E.	25.7	20.0
77	NE¼ sec. 23, T. 11 N., R. 8 E.	21.4	16.5
78	NW¼ sec. 23, T. 11 N., R. 8 E.	5.3	12.1
79	SW¼ sec. 14, T. 11 N., R. 8 E.	33.2	24.3
80	SW¼ sec. 14, T. 11 N., R. 8 E.	2.3	5.9
81	NW¼ sec. 13, T. 11 N., R. 8 E.	2.2	8.8
82	NE¼ sec. 13, T. 11 N., R. 8 E.	2.3	6.6
83	NE¼ sec. 13, T. 11 N., R. 8 E.	2.0	8.5
84	NW¼ sec. 18, T. 11 N., R. 8 E.	1.0	4.3
85	NE¼ sec. 4, T. 11 N., R. 8 E.	6.7	5.7
86	SW¼ sec. 34, T. 11 N., R. 8 E.	1.6	2.9
87	SW¼ sec. 34, T. 11 N., R. 8 E.	3.8	14.3
88	NE¼ sec. 24, T. 11 N., R. 8 E.	2.3	9.9
89	NW¼ sec. 19, T. 11 N., R. 9 E.	2.8	9.3
90	SE¼ sec. 24, T. 11 N., R. 8 E.	33.0	18.6
91	NW¼ sec. 25, T. 11 N., R. 8 E.	23.6	16.7

APPENDIX B

URANIUM IN THE NONMAGNETIC HEAVY-MINERAL FRACTION OF THE STREAM-SEDIMENT SAMPLES

APPENDIX B

URANIUM IN THE NONMAGNETIC HEAVY MINERAL FRACTION OF THE STREAM-SEDIMENT SAMPLES

Sample no.	Weight % nonmagnetic heavy minerals	cU_3O_8 (ppm)	Sample no.	Weight % nonmagnetic heavy minerals	cU_3O_8 (ppm)
1	1.70	1569	46	6.02	483
2	3.20	1000	47	0.87	755
3	11.60	62	48	0.97	539
4	2.90	438	49	13.60	2844
5	0.96	336	50	0.89	1333
6	0.86	1222	51	6.72	1210
7	2.10	900	52	1.64	427
8	1.20	638	53	5.76	1274
9	0.96	79	54	7.10	1100
10	1.47	1712	55	0.80	600
11	2.52	758	56	8.00	863
12	2.28	476	57	9.36	1105
13	2.49	4188	58	1.83	363
14	4.86	1085	59	0.95	211
15	2.22	548	60	0.83	494
16	5.67	1686	61	2.61	563
17	1.92	187	62	1.48	289
18	19.84	1469	63	2.13	473
19	1.78	664	64	7.90	300
20	2.85	669	65	2.72	785
21	1.82	97	66	14.60	664
22	1.66	1491	67	8.28	346
23	0.90	826	68	0.87	88
24	0.60	792	69	0.75	274
25	1.88	63	70	2.58	87
26	4.55	33	71	0.75	144
27	0.93	28	72	3.08	96
28	1.94	40	73	0.86	306
29	1.78	144	74	0.92	33
30	0.93	119	75	1.70	176
31	2.79	595	76	2.64	1204
32	0.93	943	77	2.85	1374
33	0.91	85	78	1.62	593
34	0.75	106	79	4.55	1813
35	0.01	48	80	1.90	1103
36	1.96	608	81	4.90	55
37	9.40	1381	82	0.94	113
38	1.80	36	83	1.84	174
39	2.46	803	84	0.95	35
40	2.58	404	85	0.83	309
41	1.94	305	86	0.90	239
42	7.83	1205	87	0.96	275
43	13.35	2879	88	2.79	342
44	2.88	642	89	1.78	267
45	1.92	841			

APPENDIX C.

GAMMA-RAY SPECTROMETRIC ANALYSES
OF ROCK SAMPLES

APPENDIX C. GAMMA-RAY SPECTROMETRIC ANALYSES OF ROCK SAMPLES

Sample No.	Location	eU ppm	eTh ppm	Rock type
1001-1	NE¼ sec. 3, T. 10 N., R. 8 E.	1.5	11.0	granite
1001-2	NE¼ sec. 3, T. 10 N., R. 8 E.	2.1	8.4	quartz monzonite pegmatite
1002-1	SE¼ sec. 34, T. 11 N., R. 8 E.	0.9	9.4	quartz monzonite
1002-2	SE¼ sec. 34, T. 11 N., R. 8 E.	5.2	6.2	granite pegmatite
1003-1	SW¼ sec. 34, T. 11 N., R. 8 E.	3.1	9.3	granite
1003-2	SW¼ sec. 34, T. 11 N., R. 8 E.	0.0	2.0	granite pegmatite
1004-1	NW¼ sec. 11, T. 11 N., R. 8 E.	0.6	7.4	granodiorite
1005-1	SW¼ sec. 11, T. 11 N., R. 8 E.	2.6	3.4	granite pegmatite
1006-1	SW¼ sec. 11, T. 11 N., R. 8 E.	5.2	24.3	quartz latite porphyry
1007-1	NW¼ sec. 18, T. 11 N., R. 9 E.	1.7	14.9	diorite porphyry
1008-1	NW¼ sec. 18, T. 11 N., R. 9 E.	2.1	16.2	granodiorite
1009-1	SW¼ sec. 18, T. 11 N., R. 9 E.	2.3	7.7	granodiorite
1010-1	NW¼ sec. 14, T. 11 N., R. 8 E.	2.3	14.0	andesite porphyry
1011-1	SW¼ sec. 14, T. 11 N., R. 8 E.	2.1	2.0	granite
1012-1	SE¼ sec. 13, T. 11 N., R. 8 E.	2.2	12.9	andesite porphyry
1013-1	SW¼ sec. 25, T. 11 N., R. 9 E.	1.6	11.6	diorite porphyry
1014-1	SW¼ sec. 14, T. 11 N., R. 8 E.	1.2	3.4	quartz diorite pegmatite
1014-2	SW¼ sec. 14, T. 11 N., R. 8 E.	2.1	15.4	quartz monzonite
1015-1	NW¼ sec. 25, T. 11 N., R. 9 E.	2.3	10.0	andesite porphyry
1016-1	NW¼ sec. 28, T. 11 N., R. 9 E.	3.3	14.1	granodiorite
1017-1	NW¼ sec. 28, T. 11 N., R. 9 E.	3.2	14.5	andesite porphyry
1018-1	NE¼ sec. 29, T. 11 N., R. 9 E.	12.4	16.9	granodiorite
1018-2	NE¼ sec. 29, T. 11 N., R. 9 E.	7.9	16.2	quartz diorite pegmatite
1019-1	NE¼ sec. 29, T. 11 N., R. 9 E.	2.8	12.6	hornblende andesite porphyry
1020-1	NE¼ sec. 29, T. 11 N., R. 9 E.	2.5	16.5	andesite porphyry
1021-1	NE¼ sec. 29, T. 11 N., R. 9 E.	1.8	10.6	hornblende diorite porphyry
1022-1	SE¼ sec. 29, T. 11 N., R. 9 E.	1.1	15.4	granodiorite
1023-1	SE¼ sec. 29, T. 11 N., R. 9 E.	1.5	10.7	granodiorite
1023-2	SE¼ sec. 29, T. 11 N., R. 9 E.	11.2	7.4	quartz diorite pegmatite
1024-1	SE¼ sec. 29, T. 11 N., R. 9 E.	1.1	11.6	quartz monzonite
1025-1	SW¼ sec. 14, T. 11 N., R. 8 E.	1.2	9.7	quartz diorite

APPENDIX C (continued)

Sample No.	Location	eU ppm	eTh ppm	Rock type
1026-1	NW¼ sec. 24, T. 11 N., R. 8 E.	12.0	1.6	granite pegmatite
1026-2	NW¼ sec. 24, T. 11 N., R. 8 E.	1.1	25.6	quartz diorite
1027-1	SW¼ sec. 23, T. 11 N., R. 8 E.	3.9	4.1	granodiorite pegmatite
1027-2	SW¼ sec. 23, T. 11 N., R. 8 E.	2.1	10.6	granite
1028-1	SW¼ sec. 23, T. 11 N., R. 8 E.	2.7	5.3	aplite
1029-1	SE¼ sec. 23, T. 11 N., R. 8 E.	2.4	15.5	quartz diorite pegmatite
1029-2	SE¼ sec. 23, T. 11 N., R. 8 E.	10.9	19.9	quartz monzonite
1029-3	SE¼ sec. 23, T. 11 N., R. 8 E.	1.8	10.7	andesite porphyry
1030-1	SE¼ sec. 26, T. 11 N., R. 8 E.	5.1	7.5	granite pegmatite
1030-2	SE¼ sec. 26, T. 11 N., R. 8 E.	14.5	13.6	quartz monzontie
1031-1	NW¼ sec. 26, T. 11 N., R. 8 E.	1.4	5.1	hornblende andesite
1032-1	NW¼ sec. 26, T. 11 N., R. 8 E.	2.5	12.7	granite
1032-2	NW¼ sec. 26, T. 11 N., R. 8 E.	2.8	9.8	granite pegmatite
1033-1	SW¼ sec. 25, T. 11 N., R. 8 E.	1.3	3.4	quartz monzonite
10033-2	SW¼ sec. 25, T. 11 N., R. 8 E.	2.0	2.2	granite pegmatite
1034-1	SW¼ sec. 25, T. 11 N., R. 8 E.	2.1	9.5	hornblende andesite porphyry
1035-1	SW¼ sec. 25, T. 11 N., R. 8 E.	2.4	5.0	granite pegmatite
1035-2	SW¼ sec. 25, T. 11 N., R. 8 E.	3.3	13.2	quartz monzonite
1035-3	SW¼ sec. 25, T. 11 N., R. 8 E.	37.0	16.7	granite pegmatite
1036-1	NW¼ sec. 30, T. 11 N., R. 9 E.	3.3	14.4	andesite porphyry
1037-1	NW¼ sec. 25, T. 11 N., R. 9 E.	2.8	13.8	hornblende andesite porphyry
1038-1	SW¼ sec. 25, T. 11 N., R. 9 E.	1.9	6.3	granite
1038-2	SW¼ sec. 25, T. 11 N., R. 9 E.	0.7	6.3	hornblende andesite
1038-3	SW¼ sec. 25, T. 11 N., R. 9 E.	3.0	13.0	andesite porphyry
1038-4	SW¼ sec. 25, T. 11 N., R. 9 E.	2.5	6.3	quartz monzonite
1038-5	SW¼ sec. 25, T. 11 N., R. 9 E.	18.1	15.1	quartz monzonite pegmatite
1038-6	SW¼ sec. 25, T. 11 N., R. 9 E.	3.4	7.8	granite
1038-7	SW¼ sec. 25, T. 11 N., R. 9 E.	2.2	13.8	andesite porphyry
1038-8	SW¼ sec. 25, T. 11 N., R. 9 E.	1.7	11.0	hornblende andesite porphyry
1039-1	NW¼ sec. 19, T. 11 N., R. 9 E.	1.7	19.1	granodiorite
1040	SW¼ sec. 25, T. 11 N., R. 9 E.	2.0	13.5	granite
1041	SE¼ sec. 25, T. 11 N., R. 9 E.	3.9	7.2	amphibolite xenolith

APPENDIX C (continued)

Sample No.	Location	eU ppm	eTh ppm	Rock type
1042	NW¼ sec. 34, T. 11 N., R. 8 E.	1.8	12.5	quartz monzonite
1043-1	SE¼ sec. 27, T. 11 N., R. 8 E.	1.9	5.4	granodiorite pegmatite
1043-2	SE¼ sec. 27, T. 11 N., R. 8 E.	1.6	10.6	quartz diorite
1044	SE¼ sec. 23, T. 11 N., R. 8 E.	2.8	12.2	andesite porphyry
1045	SE¼ sec. 23, T. 11 N., R. 8 E.	12.9	11.1	granite pegmatite
1046	SE¼ sec. 23, T. 11 N., R. 8 E.	4.1	19.2	quartz monzonite
1047	SW¼ sec. 24, T. 11 N., R. 8 E.	4.2	8.8	quartz monzonite pegmatite
1048-1	NE¼ sec. 19, T. 11 N., R. 9 E.	2.3	11.0	andesite porphyry
1048-2	NW¼ sec. 19, T. 11 N., R. 9 E.	1.5	14.5	granodiorite
1048-3	NE¼ sec. 19, T. 11 N., R. 9 E.	13.6	16.5	granite pegmatite
1048-4	NE¼ sec. 19, T. 11 N., R. 9 E.	2.8	16.2	andesite porphyry
1049-1	SE¼ sec. 19, T. 11 N., R. 9 E.	1.7	6.9	hornblende andesite
1049-2	SE¼ sec. 19, T. 11 N., R. 9 E.	1.4	11.6	granodiorite
1049-3	SE¼ sec. 19, T. 11 N., R. 9 E.	2.4	15.9	dacite porphyry
1050-1	SE¼ sec. 19, T. 11 N., R. 9 E.	1.6	13.2	granodiorite
1050-2	SE¼ sec. 19, T. 11 N., R. 9 E.	1.5	6.5	hornblende andesite
1051-1	SE¼ sec. 19, T. 11 N., R. 9 E.	3.6	5.4	amphibolite xenolith
1052-1	SE¼ sec. 18, T. 11 N., R. 9 E.	2.1	6.0	quartz monzonite
1052-2	SE¼ sec. 18, T. 11 N., R. 9 E.	2.2	11.1	andesite porphyry
1053	NE¼ sec. 14, T. 11 N., R. 8 E.	2.7	13.4	dacite porphyry
1054-1	NW¼ sec. 24, T. 11 N., R. 8 E.	22.5	15.6	granite pegmatite
1054-2	NW¼ sec. 24, T. 11 N., R. 8 E.	2.5	9.3	andesite porphyry
1054-3	NW¼ sec. 24, T. 11 N., R. 8 E.	1.2	7.9	quartz monzonite
1055	NW¼ sec. 24, T. 11 N., R. 8 E.	14.7	17.6	quartz monzonite
1056	SE¼ sec. 13, T. 11 N., R. 8 E.	2.6	8.5	andesite porphyry
1057-1	SE¼ sec. 13, T. 11 N., R. 8 E.	15.8	13.4	granite pegmatite
1057-2	SE¼ sec. 13, T. 11 N., R. 8 E.	0.9	12.2	granodiorite
1058	NE¼ sec. 24, T. 11 N., R. 8 E.	2.1	13.0	quartz diorite
1059-1	NE¼ sec. 24, T. 11 N., R. 8 E.	1.9	15.5	quartz diorite
1059-2	NE¼ sec. 24, T. 11 N., R. 8 E.	12.4	10.3	quartz diorite pegmatite
1060-1	SW¼ sec. 19, T. 11 N., R. 9 E.	11.1	12.8	granite pegmatite
1060-2	SW¼ sec. 19, T. 11 N., R. 9 E.	1.8	11.4	quartz diorite
1060-3	SW¼ sec. 19, T. 11 N., R. 9 E.	1.5	6.7	hornblende andesite prophyry
1061-1	SW¼ sec. 19, T. 11 N., R. 9 E.	5.0	22.4	quartz latite porphyry
1061-2	SW¼ sec. 19, T. 11 N., R. 9 E.	2.3	9.0	andesite porphyry

APPENDIX C (continued)

Sample No.	Location	eU ppm	eTh ppm	Rock type
1062-1	SW¼ sec. 19, T. 11 N., R. 9 E.	1.1	9.7	quartz monzonite
1062-2	SW¼ sec. 19, T. 11 N., R. 9 E.	7.7	5.6	grantie pegmatite
1063	SW¼ sec. 19, T. 11 N., R. 9 E.	1.9	13.4	granite
1064-1	SE¼ sec. 11, T. 11 N., R. 8 E.	2.0	3.2	granite pegmatite
1064-2	SE¼ sec. 11, T. 11 N., R. 8 E.	0.8	3.7	quartz monzonite
1065	SE¼ sec. 11, T. 11 N., R. 8 E.	1.6	2.3	granodiorite pegmatite
1066	SW¼ sec. 12, T. 11 N., R. 8 E.	0.2	5.9	quartz monzonite
1067-1	NE¼ sec. 23, T. 11 N., R. 8 E.	4.4	18.0	granite
1067-2	NE¼ sec. 23, T. 11 N., R. 8 E.	21.7	22.3	granite
1068-1	NE¼ sec. 23, T. 11 N., R. 8 E.	9.0	9.0	granodiorite pegmatite
1068-2	NE¼ sec. 23, T. 11 N., R. 8 E.	2.7	13.5	quartz monzonite
1069	SW¼ sec. 14, T. 11 N., R. 8 E.	2.8	14.1	quartz pegmatite
1070-1	NE¼ sec. 22, T. 11 N., R. 8 E.	0.1	3.5	quartz diorite pegmatite
1070-2	NE¼ sec. 22, T. 11 N., R. 8 E.	0.8	11.1	quartz monzonite
1070-3	NE¼ sec. 22, T. 11 N., R. 8 E.	1.7	10.9	andesite porphyry
1071-1	SE¼ sec. 26, T. 11 N., R. 8 E.	1.8	14.4	andesite porphyry
1072-1	SE¼ sec. 26, T. 11 N., R. 8 E.	3.2	10.1	quartz diorite pegmatite
1073-1	NE¼ sec. 35, T. 11 N., R. 8 E.	0.2	10.8	quartz monzonite
1073-2	NE¼ sec. 35, T. 11 N., R. 8 E.	1.9	7.0	aplite
1074-1	NE¼ sec. 35, T. 11 N., R. 8 E.	0.9	3.3	quartz pegmatite
1074-2	NE¼ sec. 35, T. 11 N., R. 8 E.	2.6	13.4	andesite porphyry
1075	SE¼ sec. 35, T. 11 N., R. 8 E.	2.7	9.9	quartz diorite
1076	SW¼ sec. 35, T. 11 N., R. 8 E.	7.0	4.2	quartz diorite pegmatite
1077-1	NW¼ sec. 35, T. 11 N., R. 8 E.	2.8	6.9	quartz diorite
1077-2	NW¼ sec. 35, T. 11 N., R. 8 E.	1.6	6.9	quartz diorite
1078	NW¼ sec. 35, T. 11 N., R. 8 E.	2.1	11.6	diorite porphyry
1079	NW¼ sec. 35, T. 11 N., R. 8 E.	2.3	16.7	andesite porphyry
1080	NW¼ sec. 35, T. 11 N., R. 8 E.	4.9	5.5	granite pegmatite
1081-1	NW¼ sec. 35, T. 11 N., R. 8 E.	1.8	7.0	quartz diorite
1081-2	NW¼ sec. 35, T. 11 N., R. 8 E.	1.6	7.1	quartz diorite
1082	NE¼ sec. 34, T. 11 N., R. 8 E.	2.2	4.2	granite pegmatite
1083	NE¼ sec. 34. T. 11 N., R. 8 E.	1.9	6.8	quartz monzonite
1084	NE¼ sec. 34, T. 11 N., R. 8 E.	0.0	0.4	quartz pegmatite
1085	NE¼ sec. 34, T. 11 N., R. 8 E.	0.7	10.3	granodiorite

APPENDIX C (continued)

Sample No.	Location	eU ppm	eTh ppm	Rock type
1086-1	SW¼ sec. 26, T. 11 N., R. 8 E.	4.2	7.5	quartz diorite pegmatite
1086-2	SW¼ sec. 26, T. 11 N., R. 8 E.	2.3	18.2	diorite porphyry
1087	SW¼ sec. 26, T. 11 N., R. 8 E.	1.1	4.7	quartz diorite pegmatite
1088-1	SW¼ sec. 26, T. 11 N., R. 8 E.	1.9	8.0	granite pegmatite
1088-2	SW¼ sec. 26, T. 11 N., R. 8 E.	4.8	9.1	aplite
1089	SW¼ sec. 26, T. 11 N., R. 8 E.	2.7	14.6	andesite porphyry
1090-1	SE¼ sec. 26, T. 11 N., R. 8 E.	1.2	8.9	andesite
1090-2	SE¼ sec. 26, T. 11 N., R. 8 E.	2.2	10.0	granite
1090-3	SE¼ sec. 26, T. 11 N., R. 8 E.	3.2	18.1	andesite porphyry
1091	NE¼ sec. 26, T. 11 N., R. 8 E.	2.4	15.2	andesite porphyry
1092	NE¼ sec. 26, T. 11 N., R. 8 E.	2.9	5.1	quartz diorite pegmatite
1093	NW¼ sec. 26, T. 11 N., R. 8 E.	2.1	7.1	granite
1094-1	NW¼ sec. 26, T. 11 N., R. 8 E.	2.7	3.3	quartz diorite pegmatite
1094-2	NW¼ sec. 26, T. 11 N., R. 8 E.	1.9	2.5	quartz monzonite
1095-1	NW¼ sec. 26, T. 11 N., R. 8 E.	2.2	10.3	quartz monzonite
1095-2	NW¼ sec. 26, T. 11 N., R. 8 E.	0.9	6.6	granite pegmatite
1096	NW¼ sec. 26, T. 11 N., R. 8 E.	1.6	2.8	granite
1097-1	SW¼ sec. 23, T. 11 N., R. 8 E.	1.8	5.8	granite
1097-2	SW¼ sec. 23, T. 11 N., R. 8 E.	7.0	5.0	quartz diorite pegmatite
1098-1	SE¼ sec. 23, T. 11 N., R. 8 E.	1.5	15.6	quartz monzonite
1098-2	SE¼ sec. 23, T. 11 N., R. 8 E.	2.2	4.4	quartz diorite pegmatite
1099	SW¼ sec. 23, T. 11 N., R. 8 E.	93.1	32.5	quartz monzonite
1100-1	SW¼ sec. 23, T. 11 N., R. 8 E.	3.3	3.3	granite pegmatite
1100-2	SW¼ sec. 23, T. 11 N., R. 8 E.	2.8	8.0	granite
1100-3	SW¼ sec. 23, T. 11 N., R. 8 E.	2.9	18.2	diorite porphyry
1101-1	NW¼ sec. 23, T. 11 N., R. 8 E.	0.9	2.1	quartz monzonite pegmatite
1101-2	NW¼ sec. 23, T. 11 N., R. 8 E.	1.5	12.0	quartz monzonite
1102	NW¼ sec. 23, T. 11 N., R. 8 E.	3.4	4.0	quartz monzonite
1103	NW¼ sec. 23, T. 11 N., R. 8 E.	5.1	11.7	granite
1104	NW¼ sec. 23, T. 11 N., R. 8 E.	1.8	2.6	quartz diorite pegmatite
1105	NW¼ sec. 19, T. 11 N., R. 9 E.	2.6	8.7	granite
1106-1	SW¼ sec. 13, T. 11 N., R. 8 E.	1.4	10.5	granodiorite
1106-2	SW¼ sec. 13, T. 11 N., R. 8 E.	3.3	5.5	quartz monzonite pegmatite

APPENDIX C (continued)

Sample No.	Location	eU ppm	eTh ppm	Rock type
1107-1	SE¼ sec. 13, T. 11 N., R. 8 E.	1.9	10.5	andesite porphyry
1107-2	SE¼ sec. 13, T. 11 N., R. 8 E.	5.9	2.8	granodiorite pegmatite
1108	SW¼ sec. 24, T. 11 N., R. 8 E.	33.0	18.6	quartz monzonite
1109	NW¼ sec. 24, T. 11 N., R. 8 E.	2.5	13.6	quartz diorite
1110-1	SW¼ sec. 24, T. 11 N., R. 8 E.	4.4	15.7	quartz monzonite
1110-2	SW¼ sec. 24, T. 11 N., R. 8 E.	3.0	4.3	quartz monzonite pegmatite
1111-1	SW¼ sec. 24, T. 11 N., R. 8 E.	18.0	14.9	quartz monzonite
1111-2	SW¼ sec. 24, T. 11 N., R. 8 E.	15.0	9.8	granite pegmatite
1112	NW¼ sec. 24, T. 11 N., R. 8 E.	2.6	13.7	quartz monzonite
1113-1	NE¼ sec. 23, T. 11 N., R. 8 E.	23.6	16.7	granite pegmatite
1113-2	NE¼ sec. 23, T. 11 N., R. 8 E.	3.5	16.0	quartz monzonite
1114-1	NE¼ sec. 23, T. 11 N., R. 8 E.	4.1	12.7	quartz monzonite
1114-2	NE¼ sec. 23, T. 11 N., R. 8 E.	2.7	5.5	granite pegmatite
1115-1	SE¼ sec. 14, T. 11 N., R. 8 E.	2.9	11.7	dacite porphyry
1116-1	SE¼ sec. 14, T. 11 N., R. 8 E.	0.7	2.8	quartz diorite pegmatite
1116-2	SE¼ sec. 14, T. 11 N., R. 8 E.	2.8	14.2	quartz monzonite
1117-1	SE¼ sec. 14, T. 11 N., R. 8 E.	7.1	11.2	quartz diorite
1118-1	SE¼ sec. 14, T. 11 N., R. 8 E.	2.0	11.5	quartz monzonite pegmatite
1118-2	SE¼ sec. 14, T. 11 N., R. 8 E.	8.5	10.1	quartz monzonite pegmatite
1119	NE¼ sec. 14, T. 11 N., R. 8 E.	3.3	10.6	andesite porphyry
1120-1	NW¼ sec. 14, T. 11 N., R. 8 E.	4.4	13.5	andesite porphyry
1120-2	NW¼ sec. 14, T. 11 N., R. 8 E.	1.6	9.0	andesite porphyry
1120-3	NW¼ sec. 14, T. 11 N., R. 8 E.	2.2	7.4	granite
1120-4	NW¼ sec. 14, T. 11 N., R. 8 E.	1.2	1.1	quartz monzonite pegmatite
1121-1	NW¼ sec. 14, T. 11 N., R. 8 E.	3.8	10.8	andesite porphyry
1122-1	SE¼ sec. 15, T. 11 N., R. 8 E.	18.1	8.6	granodiorite
1122-2	SE¼ sec. 15, T. 11 N., R. 8 E.	1.1	13.3	granite pegmatite
1123-1	NE¼ sec. 25, T. 11 N., R. 8 E.	.0	.0	quartz pegmatite
1124-1	SW¼ sec. 24, T. 11 N., R. 8 E.	2.3	13.3	quartz monzonite
1125-1	SW¼ sec. 24, T. 11 N., R. 8 E.	2.1	20-4	granite
1126-1	SW¼ sec. 24, T. 11 N., R. 8 E.	5.1	5.5	aplite
1126-2	SW¼ sec. 24, T. 11 N., R. 8 E.	2.6	11.3	andesite porphyry
1126-3	SW¼ sec. 24, T. 11 N., R. 8 E.	0.2	.0	quartz pegmatite

APPENDIX C (continued)

Sample No.	Location	eU ppm	eTh ppm	Rock type
1127-1	SE¼ sec. 23, T. 11 N., R. 8 E.	1.6	12.3	granite
1127-2	SE¼ sec. 23, T. 11 N., R. 8 E.	9.6	7.5	quartz diorite pegmatite
1128-1	NE¼ sec. 26, T. 11 N., R. 8 E.	2.6	13.8	quartz latite porphyry
1128-2	NE¼ sec. 26, T. 11 N., R. 8 E.	1.1	2.1	quartz monzonite pegmatite
1129-1	NE¼ sec. 26, T. 11 N., R. 8 E.	1.9	9.4	granite
1129-2	NE¼ sec. 26, T. 11 N., R. 8 E.	1.1	12.3	quartz monzonite pegmatite
1130-1	SW¼ sec. 25, T. 11 N., R. 8 E.	1.4	15.1	quartz monzonite
1130-2	SW¼ sec. 25, T. 11 N., R. 8 E.	0.6	5.6	granite pegmatite
1131-1	NW¼ sec. 25, T. 11 N., R. 8 E.	3.8	17.5	quartz monzonite
1132-1	SW¼ sec. 25, T. 11 N., R. 8 E.	1.4	13.2	quartz monzonite
1133-1	NE¼ sec. 26, T. 11 N., R. 8 E.	1.8	12.0	granite
1134-1	SW¼ sec. 25, T. 11 N., R. 8 E.	7.5	7.7	aplite
1135-1	SW¼ sec. 25, T. 11 N., R. 8 E.	1.6	14.0	quartz monzonite
1136-1	SE¼ sec. 26, T. 11 N., R. 8 E.	1.9	10.7	granite
1136-2	SE¼ sec. 26, T. 11 N., R. 8 E.	1.3	6.8	quartz diorite pegmatite
1136-3	SE¼ sec. 26, T. 11 N., R. 8 E.	1.4	5.8	quartz monzonite pegmatite
1137-1	SE¼ sec. 26, T. 11 N., R. 8 E.	5.1	12.3	grante pegmatite
1137-2	SE¼ sec. 26, T. 11 N., R. 8 E.	1.7	8.6	granite
1138-1	SE¼ sec. 26, T. 11 N., R. 8 E.	2.5	8.1	quartz monzonite
1139-1	SW¼ sec. 26, T. 11 N., R. 8 E.	1.9	9.7	granite
1139-2	SW¼ sec. 26, T. 11 N., R. 8 E.	1.4	4.2	quartz diorite pegmatite
1140-1	SW¼ sec. 26, T. 11 N., R. 8 E.	3.3	13.9	andesite porphyry
1141-1	NE¼ sec. 34, T. 11 N., R. 8 E.	0.8	11.1	granodiorite
1141-2	NE¼ sec. 34, T. 11 N., R. 8 E.	5.7	3.6	quartz monzonite pegmatite
1142-1	NE¼ sec. 4, T. 10 N., R. 8 E.	4.3	7.1	andesite porphyry
1143-1	SW¼ sec. 34, T. 11 N., R. 8 E.	3.0	16.1	quartz diorite
1144-1	NW¼ sec. 3, T. 10 N., R. 8 E.	6.9	11.6	quartz monzonite
1145-1	NW¼ sec. 3, T. 10 N., R. 8 E.	5.5	9.3	quartz monzonite
1145-2	NW¼ sec. 3, T. 10 N., R. 8 E.	3.0	1.9	granite pegmatite
1146-1	SW¼ sec. 34, T. 11 N., R. 8 E.	5.6	5.0	granite pegmatite

APPENDIX D

DESCRIPTIONS OF LITHOLOGIES

APPENDIX D

DESCRIPTIONS OF LITHOLOGIES

QUARTZ PEGMATITES

A total of five (5) samples were identified as quartz pegmatites, consisting predominantly of quartz with lesser amounts of plagioclase, K-feldspar, muscovite-sericite, zircon, opaque minerals, and biotite. All five samples are medium to coarse grained, holocrystalline, and allotriomorphic.

Quartz (91 to 98%) occurs predominantly as medium to coarse single anhedral grains displaying moderate to strong undulose extinction which gives them a semicomposite appearance. Quartz-to-quartz contacts for single anhedral grains range from smooth to sutured and crenulated. Polycrystalline and stretched grains occur in minor amounts. The polycrystalline grains have a recrystallized metamorphic texture consisting of equant interlocking grains with straight boundaries and slightly undulose extinction. The stretched grains are composed of somewhat elongate lenticular crystal units that have smooth to crenulated boundaries. The presence of the polycrystalline and stretched quartz suggests that some of the pegmatites were subjected to deformational stresses with some recrystallization. Inclusions of muscovite-sericite were observed in all types of quartz grains. In addition to the above-mentioned occurrences, quartz also occurs in thin secondary veins, commonly associated with sericite and iron oxides. Plagioclase and K-feldspar (0 to 3%) were observed only in sample 1069 as small anhedral grains that appear to be fresh. Inclusions of muscovite were observed within both feldspars. The plagioclase grains show minor strain features as evidenced by slightly bent twin lamellae. Muscovite and (or) sericite (1 to 7%) occur predominantly as small thin flakes between quartz grains and, less frequently, as small inclusions within quartz grains. Opaque minerals (0 to 1%) occur both as subhedral to anhedral grains disseminated throughout the samples and as extremely fine anhedral grains associated with quartz and sericite in thin secondary veins. Zircon and biotite occur in trace amounts as inclusions within quartz grains.

APLITES

A total of five (5) samples were identified as aplites composed primarily of quartz, plagioclase, and K-feldspar with lesser amounts of muscovite, biotite, opaque minerals, zircon, and allanite. All five aplites are fine grained, holocrystalline, allotriomorphic, and saccharoidal (granular).

Quartz (25 to 48%) is the dominant mineral in most of the aplites and occurs as small anhedral grains. Quartz can be seen to embay and engulf grains of plagioclase and K-feldspar and is itself engulfed by plagioclase and K-feldspar. Inclusions of muscovite, biotite, rutile, zircon, allanite, and opaque minerals were observed within the quartz grains. Plagioclase (20 to 30%) (andesine-oligoclase) occurs as small anhedral grains, showing trace to minor alteration to kaolinite. A few plagioclase grains are bordered by myrmekite. Inclusions of muscovite, biotite, zircon, and opaque minerals were observed. K-feldspar (30 to 49%) (microcline, microcline-perthite, orthoclase) also occurs as small anhedral grains showing trace amounts of alteration to kaolinite-sericite. Inclusions of muscovite, biotite, zircon, opaque minerals, and allanite were observed within K-feldspar grains. Muscovite (tr to 1%) and biotite (tr to 1%) are present, both as inclusions within quartz, plagioclase, and K-feldspar and as interstitial grains (flakes) disseminated throughout the samples. Opaque minerals occur in trace amounts as anhedral to subhedral grains, disseminated interstitially within the samples and also as inclusions within other mineral grains. Zircon and allanite occur in trace amounts within the samples, primarily as inclusions within quartz and K-feldspar grains and also as interstitial grains.

GRANODIORITE PEGMATITES

A total of five (5) samples were identified as granodiorite pegmatites consisting predominantly of quartz and plagioclase with lesser and variable amounts of K-feldspar, muscovite-sericite, biotite, zircon, epidote, garnet, and opaque minerals. All five samples are medium to coarse grained, holocrystalline, and allotriomorphic.

Quartz (33 to 57%) occurs predominantly as medium- to coarse-grained, single anhedral grains, displaying slight to moderate undulose extinction. Quartz grain boundaries are predominantly smooth but sutured and crenulated contacts were also observed. The presence of some stretched quartz that displays strong undulose extinction suggests that some of the granodiorite pegmatites were subjected to deformational stresses with an absence of recrystallization. Inclusions of plagioclase, K-feldspar, muscovite-sericite, biotite, zircon, garnet, and opaque minerals were observed within quartz grains. Plagioclase (30 to 47%) occurs as medium- to coarse-grained, anhedral to subhedral grains. Alteration of plagioclase to kaolinite ranges from minor to moderate, with the majority showing only minor alteration. The presence of curved and (or) offset twin lamellae within the plagioclase grains suggests that these pegmatites were subjected to deformational stresses. Inclusions of muscovite-sericite, opaque minerals, quartz, garnet, biotite, plagioclase, and K-feldspar were observed within the plagioclase grains. K-feldspar (6 to 15%) occurs as anhedral grains of microcline and microcline-perthite displaying only trace amounts of alteration to kaolinite-sericite. Inclusions of quartz, plagioclase, muscovite-sericite, garnet, biotite, and opaque minerals were observed within K-feldspar grains. Muscovite and its fine-grained equivalent sericite (0 to 8%) occur both as disseminated interstitial grains and as inclusions within other mineral grains. Quartz, garnet, and opaque minerals are common inclusions within muscovite grains. Biotite (0 to 2%) was observed in association with muscovite and as inclusions within other mineral grains. Zircon, epidote, and opaque minerals occur in trace amounts disseminated throughout the samples. Garnet (tr to 1%) occurs as subhedral to euhedral grains in disseminated form as interstitial grains or inclusions, and as clusters or aggregates of grains.

QUARTZ DIORITE PEGMATITES

In all, eighteen (18) samples were identified as quartz diorite pegmatites and consist predominantly of quartz and plagioclase with lesser and variable amounts of K-feldspar, muscovite-sericite, biotite, zircon, apatite, chlorite-penninite, epidote, garnet, and opaque minerals. Texturally, all the quartz diorite pegmatite samples are medium to coarse grained, holocrystalline, and allotriomorphic.

Quartz (15 to 84%) occurs predominantly as medium grained, single anhedral grains, displaying slight to moderate undulose extinction giving them a semicomposite appearance. Quartz grain boundaries are predominantly smooth but sutured-crenulated appearing contacts were also observed. As is the case with the quartz pegmatites, the presence of some stretched quartz displaying strong undulose extinction suggests that some of the quartz diorite pegmatites were subjected to deformational stresses with an absence of recrystallization. Inclusions of plagioclase, K-feldspar, muscovite-sericite, biotite, zircon, chlorite-penninite, garnet, and opaque minerals were observed within quartz grains. Plagioclase (13 to 83%) occurs as medium- to coarse-grained, anhedral to subhedral grains. Although not very common, zonation was observed in some plagioclase grains. Alteration of plagioclase feldspar to kaolinite ranges from minor to moderate with the majority of plagioclase grains showing only minor alteration. Curved and (or) offset twin lamellae were frequently observed and as with the stretched quartz suggest that these pegmatites were subjected to deformational stresses. Inclusions of muscovite-sericite, opaque minerals, quartz, garnet, biotite, plagioclase, and microcline were observed within the plagioclase grains. K-feldspar (0 to 5%) (microcline and microcline-perthite) occurs as anhedral grains displaying only trace amounts of alteration to kaolinite. Inclusions of quartz, plagioclase, muscovite-sericite, garnet, biotite, and opaque minerals were frequently observed within K-feldspar grains. Muscovite (0 to 12%) and its fine-grained equivalent sericite occur both as disseminated interstitial grains and as inclusions within other mineral grains. Occasionally, muscovite occurs as an aggregate or cluster of individual grains. Quartz, garnet, and opaque minerals are common inclusions within muscovite grains. Biotite (0 to 1%), which is not as common as muscovite-sericite in the quartz diorite pegmatites, occurs in association with muscovite aggregates or as inclusions within quartz and feldspar grains. Zircon, apatite, chlorite-penninite, epidote, and opaque minerals occur in trace amounts disseminated throughout the samples as interstitial grains or as inclusions within other mineral grains. In addition to the above-mentioned occurrences, opaque minerals (iron oxides) were also observed as fracture fillings or as alteration rims on garnet grains. Garnet (0 to 2%) occurs as subhedral to euhedral grains in disseminated form as interstitial grains or inclusions and as clusters or aggregates of grains.

"PNEUMATOLYTIC" QUARTZ DIORITE PEGMATITE

Sample 1014-1 was identified as a "pneumatolytic" quartz diorite pegmatite composed of quartz, plagioclase, K-feldspar, muscovite-sericite, biotite, amphiboles, zircon, garnet, tourmaline, fluorite, epidote, apatite, topaz, rutile, and opaque minerals. Texturally, the sample is medium to coarse grained, holocrystalline, and hypidiomorphic.

Quartz (32%) occurs as anhedral grains containing few inclusions. Some quartz appears to be secondary in nature as evidenced by podlike shapes. Plagioclase (45%) occurs as anhedral to subhedral grains showing moderate alteration to kaolinite and occasional zonation. Inclusions of muscovite-sericite, biotite, opaque minerals, zircon, and garnet were observed within plagioclase grains. A few plagioclase grains are extensively fractured with the fractures being filled in with iron oxides. K-feldspar (microcline) occurs in trace amounts as moderately altered anhedral grains disseminated throughout the sample. Muscovite-sericite (7%) and biotite (5%) occur as flakes of variable size both interstitially disseminated throughout the sample and as inclusions within other mineral grains. Zircon, garnet, an unidentified amphibole, tourmaline, epidote, rutile, and apatite occur primarily as trace inclusions within quartz, feldspar, muscovite, and biotite and less frequently as interstitial grains. Fluorite (3%) and topaz (4%) occur in close association with one another as interstitial grains disseminated throughout the sample. Opaque minerals (1%) (iron oxides) occur along grain boundaries and fractures and as irregular masses in the sample.

QUARTZ MONZONITE PEGMATITES

A total of thirteen (13) samples were identified as quartz monzonite pegmatites. Quartz, plagioclase, and K-feldspar are the predominant constituents with muscovite-sericite, biotite, zircon, epidote, tourmaline, garnet, apatite, allanite, and opaque minerals present in lesser and variable amounts. Texturally, the quartz monzonite pegmatite samples are predominantly medium to coarse grained, holocrystalline, and allotriomorphic to hypidiomorphic.

Quartz (15 to 57%) occurs as anhedral grains which show minor to moderate undulatory extinction. As in the other pegmatites, some quartz shows stretch features which suggests that the quartz monzonite pegmatites were subjected to deformational stresses with an absence of recrystallization. Inclusions of plagioclase, K-feldspar, muscovite-sericite, biotite, zircon, tourmaline, garnet, apatite, and opaque minerals were observed within quartz grains. Plagioclase (22 to 45%) (oligoclase and andesine) occurs as anhedral to subhedral grains and inclusions displaying trace to moderate alteration to kaolinite. In some cases, alteration was confined strictly to cleavage traces. Minor amounts of zoned plagioclase were observed in all the samples. Inclusions are common within the plagioclase grains with muscovite-sericite, biotite, zircon, garnet and opaque minerals being the most common. Curved and (or) offset twin lamellae within some plagioclase grains are indicative of deformational stresses. K-feldspar (10 to 45%) (microcline, microcline-perthite, and orthoclase) occurs as relatively fresh anhedral grains. All three varieties of K-feldspar contain inclusions of or poikilitically enclose plagioclase, quartz, muscovite-sericite, biotite, zircon, garnet, and opaque minerals. Sample 1101-1 contains what appears to be second generation microcline which poikilitically encloses numerous mineral grains. Muscovite-sericite (tr to 20%) and biotite (0 to 3%) occur as flakes of variable size disseminated interstitially throughout the sample and as inclusions within other mineral grains. Occasionally, clusters or aggregates of muscovite-sericite and biotite were observed. Zircon, epidote, tourmaline, apatite, allanite and opaque minerals occur in trace amounts both as inclusions in other mineral grains and as interstitial grains. In addition, opaque minerals (iron oxides) occur as thin fracture fillings and as alteration rims on garnet grains. Garnet (0 to 2%) occurs as subhedral to euhedral grains in disseminated form as interstitial grains and as inclusions within other minerals and as clusters or aggregates of grains.

GRANITE PEGMATITES

A total of twenty-nine (29) samples were identified as granite pegmatites. Quartz, K-feldspar, and plagioclase are the primary constituents with muscovite-sericite, biotite, chlorite-penninite, sphene, apatite, epidote, fluorite, allanite, zircon, garnet, and opaque minerals present in lesser and variable amounts. Texturally, the granite pegmatite samples are coarse grained, holocrystalline, and allotriomorphic. A few samples show variation in grain size with K-feldspar grains being larger than other mineral grains in the sample. Graphic textures were observed in some samples.

Quartz (1 to 50%) occurs predominantly as single anhedral grains and to a lesser extent as cuneiform inclusions in graphic granite pegmatites, myrmekitic inclusions in microcline, and as stretched grains. The presence of trace amounts of stretched quartz indicates that some granite pegmatites were subjected to deformational stresses with an absence of recrystallization. Inclusions of plagioclase, K-feldspar, muscovite, garnet, opaque minerals, biotite, apatite, zircon, and allanite were observed. A few samples contained quartz grains which were fractured and filled in with iron oxides. K-feldspar (30 to 93%) (microcline, microcline-perthite, and orthoclase) occurs as anhedral grains which are usually larger than the other minerals in the sample. In some samples the K-feldspar grains are so large that they poikilitically enclose most other mineral grains. As previously mentioned, myrmekitic and graphic textures are common in the granite pegmatites. Perthitic intergrowths of K-feldspar and plagioclase are also well developed. Most K-feldspar grains are relatively fresh showing only trace to minor amounts of alteration to kaolinite-sericite In some cases, alteration can be observed only along cleavage traces. Inclusions of subhedral plagioclase, quartz, garnet, muscovite, biotite, opaque minerals, apatite, and zircon were commonly observed. Plagioclase (tr to 25%) (oligoclase-andesine) occurs both as anhedral grains and as subhedral to euhedral inclusions in K-feldspar. Generally, the plagioclase grains are smaller than K-feldspar grains. Graphic intergrowths of quartz with plagioclase were occasionally observed. Some plagioclase inclusions show compositional zonation with the inner zone (probably more calcic) being more altered than the external zone. Most plagioclase grains show trace to minor amounts of alteration. Inclusions of quartz, muscovite, garnet, and apatite were occasionally observed. Muscovite-sericite (tr to 6%) and biotite (0 to 2%) occur as flakes of variable size disseminated throughout the sample either singularly or in clusters and as inclusions within other mineral grains. Occasionally, epidote (0 to tr) is associated with muscovite. In addition to the above-mentioned occurrences, muscovite was also observed as a fracture filling within large microcline grains. The primary occurrence of apatite, zircon, opaque minerals, and allanite is as trace inclusions in other mineral grains although all were also observed as interstitial grains. Fluorite (trace) was observed only in sample 1095-2 where it occurs as inclusions in microcline grains. Garnet occurs as subhedral to euhedral grains both interstitially and as inclusions in other minerals. Occasional clusters or aggregates of garnet grains were observed.

QUARTZ DIORITES

A total of nine (9) samples were found to be quartz diorites. The samples consist primarily of quartz and plagioclase with lesser and variable amounts of K-feldspar, muscovite-sericite, biotite, chlorite-penninite, sphene, apatite, zircon, tourmaline, epidote, allanite, monazite, and opaque minerals. Texturally, the samples are predominantly medium grained, holocrystalline, and hypidiomorphic.

Quartz (22 to 30%) occurs predominantly as single anhedral grains and to a lesser extent as secondary fracture fillings and stretched grains. Slight to moderate undulose extinction is common and thus gives some quartz grains a semicomposite appearance. The presence of some stretched quartz suggests that some quartz diorites were subjected to deformational stresses. Inclusions of muscovite-sericite, biotite, plagioclase, K-feldspar, epidote, allanite, opaque minerals, sphene, tourmaline, apatite, and zircon were observed. Plagioclase (45 to 68%) occurs as anhedral to subhedral grains which display variable degrees of alteration to kaolinite. Zonation was observed in some samples and occasionally resulted in the calcic core being more altered than the external portions of the plagioclase grain. On a few grains, a myrmekitic intergrowth of quartz and plagioclase was observed near grain extremities. Inclusions of quartz, biotite, muscovite-sericite, chlorite-penninite, epidote, opaque minerals, allanite, apatite, zircon, sphene, and monazite were observed. K-feldspar (0 to 5%) (microcline, microcline-perthite, orthoclase) occurs as anhedral grains which also show variable amounts of alteration to kaolinite-sericite (trace to extensive). Myrmekitic intergrowths of quartz and K-feldspar were occasionally observed. Inclusions of quartz, plagioclase, muscovite-sericite, chlorite-penninite, biotite, sphene, apatite, epidote, allanite, monazite, and opaque minerals were frequently observed. Muscovite-sericite (0 to 1%) occurs predominantly in trace amounts disseminated throughout the samples as interstitial flakes and as inclusions in other minerals. Muscovite also occurs as intergrowths with biotite. Biotite (2 to 10%) is far more abundant than muscovite in these samples. It occurs both as single flakes of variable size or as aggregates of flakes. Allanite, which occurs as euhedral zoned grains with epidote rims, is commonly found in trace amounts as inclusions in biotite, where it displays radioactive halos. Chlorite-penninite (0 to 3%) occurs as interstitial flakes and occasionally as fracture fillings within some samples. Sphene (0 to tr) occurs both as acute rhombic crystals and in massive form. Some sphene grains are coated with opaque minerals. Apatite, zircon, and tourmaline occur in trace amounts predominantly as inclusions within other mineral grains. Epidote (0 to 8%) occurs as interstitial grains, as rims on allanite grains, and as inclusions in other mineral grains. Monazite was tentatively identified in several samples where it occurs in trace amounts as zoned subhedral grains commonly associated with apatite and rhombic opaque minerals. Opaque minerals (tr to 5%) have anhedral to euhedral outlines and occasional rhombic and cubic forms. Iron oxides are common in some samples as fracture fillings.

ALTERED AND DEFORMED QUARTZ DIORITES

Although samples 1025-1 and 1117-1 were tentatively identified as quartz diorites, both were found to be quite different from those described in the preceding section. Both were found to consist predominantly of plagioclase and quartz with lesser amounts of K-feldspar, muscovite, biotite, zircon, apatite, and opaque minerals. Texturally, both samples are medium grained, holocrystalline, and hypidiomorphic.

Quartz (39 to 55%) commonly occurs as anhedral, stretched, sutured, and crenulated grains. The nature and appearance of the quartz suggests that these samples were subjected to deformational stresses with some recrystallization. Plagioclase (35 to 45%) occurs as anhedral to subhedral grains, the majority of which show extensive alteration to kaolinite-sericite. K-feldspar (0 to 5%) (microcline, perthite) occurs as anhedral grains which show minor to moderate alteration. Muscovite (8 to 10%) occurs as small flakes commonly found around larger mineral grains in the sample. Biotite, zircon, apatite, and opaque minerals occur in trace amounts disseminated throughout the sample.

GRANODIORITES

A total of nineteen (19) samples were found to be granodiorites. The samples consist primarily of quartz and plagioclase with lesser and variable amounts of K-feldspar, muscovite-sericite, biotite, chlorite-penninite, sphene, apatite, zircon, tourmaline, epidote, allanite, monazite, and opaque minerals. Texturally, the samples are predominantly medium grained, holocrystalline, and hypidiomorphic.

Quartz (25 to 50%) occurs predominantly as single anhedral grains and to a lesser extent as secondary fracture fillings and stretched grains. Slight to moderate undulose extinction is common. The presence of some stretched quartz suggests that some granodiorites were subjected to deformational stresses. Inclusions of muscovite-sericite, biotite, plagioclase, K-feldspar, epidote, allanite, opaque minerals, sphene, tourmaline, apatite, and zircon were observed. Plagioclase (30 to 60%) occurs as anhedral to subhedral grains displaying variable degrees of alteration to kaolinite. Faint zonation was observed in some samples. Myrmekitic intergrowths of quartz and plagioclase were observed near the extremities of some grains. Inclusions of quartz, biotite, muscovite-sericite, chlorite-penninite, epidote, opaque minerals, allanite, apatite, zircon, sphene, and monazite were observed within plagioclase grains. K-feldspar (4 to 15%) (microcline, microcline-perthite, orthoclase) occurs as anhedral grains which show variable (trace to extensive) alteration to kaolinite-sericite. Myrmekitic intergrowths of quartz and K-feldspar were frequently observed. Inclusions of quartz, plagioclase, muscovite-sericite, chlorite-penninite, biotite, sphene, apatite, epidote, allanite, monazite, and opaque minerals were observed within K-feldspar grains. Muscovite-sericite (0 to 3%) occurs disseminated throughout the samples as interstitial flakes and as inclusions within other minerals. Muscovite also occurs intergrown with biotite. Biotite (0 to 13%) occurs both as single flakes and as aggregates of flakes. Allanite occurs in trace amounts as euhedral zoned grains with epidote rims. As inclusions within biotite, allanite displays distinct radioactive halos. Chlorite-penninite (0 to 2%) occurs as interstitial flakes and occasionally as fracture fillings. Sphene (0 to 3%) occurs both as acute rhombic crystals and in massive form. Apatite, zircon, and tourmaline occur in trace amounts predominantly as inclusions within other mineral grains. Epidote (0 to 6%) occurs as interstitial grains, as rims on allanite grains, and as inclusions in other mineral grains. Monazite occurs in trace amounts as zoned subhedral grains commonly associated with apatite and rhombic opaque minerals. Opaque minerals (tr to 4%) occur in disseminated form as subhedral to euhedral grains.

QUARTZ MONZONITES

A total of forty-one (41) samples were identified as quartz monzonites. Quartz, plagioclase, and K-feldspar are the main components with muscovite-sericite, biotite, chlorite-penninite, allanite, sphene, epidote, fluorite, apatite, zircon, and opaque minerals present in lesser and variable amounts. Texturally, the samples are predominantly medium grained, holocrystalline, and allotriomorphic to hypidiomorphic. The majority of the quartz monzonites could be called leucomonzonites.

Quartz (15 to 49%) occurs predominantly as single anhedral grains and to a lesser extent as stretched grains. Slight to moderate undulose extinction is common giving some quartz grains a semicomposite appearance. Inclusions of zircon, apatite, rutile, biotite, allanite, and opaque minerals were observed. Plagioclase (18 to 40%) occurs as anhedral to subhedral grains which are generally smaller in size than K-feldspar grains.

Alteration to kaolinite is variable in extent, ranging from trace to moderate. Some plagioclase grains show zonation, with internal more calcic zones being more altered than the outer zones. A few samples contain plagioclase grains with bent-curved and (or) offset twin lamellae suggesting that the samples were subjected to deformational stresses. Inclusions of biotite, muscovite-sericite, plagioclase, zircon, allanite, epidote, sphene, and opaque minerals were observed. K-feldspar (16 to 44%) (microcline, orthoclase, and microcline-perthite) occurs as anhedral grains which show trace to minor alteration to kaolinite-sericite. Myrmekitic intergrowths with quartz were occasionally observed. Inclusions of plagioclase, quartz, biotite, muscovite, apatite, sphene, allanite, epidote, and opaque minerals were frequently observed. Muscovite-sericite (0 to 15%) occurs as flakes of variable size disseminated throughout the samples. It also occurs as small flakes along grain boundaries of other minerals. Muscovite-sericite is commonly associated with biotite and frequently contains inclusions of quartz, zircon, and opaque minerals. Biotite (tr to 14%) also occurs as flakes of variable size disseminated throughout the samples. It is commonly associated with and contains inclusions of opaque minerals, sphene, muscovite, apatite, epidote, chlorite-penninite, fluorite, and allanite. Chlorite-penninite (0 to 4%) occurs as distinct grains, as a fracture filling with opaque minerals, and as an alteration product of biotite. Allanite (0 to tr) occurs as euhedral-zoned inclusions within biotite, plagioclase, and K-feldspar. When it occurs as an inclusion within biotite, radioactive halos are commonly observed. Sphene, apatite, epidote, fluorite, and zircon occur in trace amounts both disseminated interstitially within the samples and as inclusions within other mineral grains. Opaque minerals occur as anhedral to euhedral grains and masses disseminated throughout the samples and as fracture fillings with chlorite-penninite.

GRANITES

A total of twenty-six (26) samples were found to be granites. Quartz, K-feldspar, and plagioclase are the principal constituents with muscovite-sericite, biotite, chlorite-penninite, allanite, epidote, sphene, fluorite, tourmaline, zircon, apatite, and opaque minerals present in lesser and variable amounts. Texturally, the granites are medium to coarse grained, holocrystalline, and allotriomorphic to hypidiomorphic.

Quartz (10 to 47%) occurs predominantly as anhedral single grains displaying slight to moderate undulatory extinction. Several grains were observed which had stretched features suggesting that some of the granites were subjected to deformational stresses. Inclusions of zircon, biotite, rutile, apatite, allanite, and opaque minerals were occasionally observed. The K-feldspar (30 to 84%) content consists mostly of microcline and microcline-perthite with lesser amounts of orthoclase, all of which are dominantly anhedral. K-feldspar grains are relatively fresh with alteration to kaolinite-sericite ranging from trace to minor. Myrmekitic and graphic intergrowths with quartz were occasionally encountered. Inclusions of quartz, biotite, muscovite, plagioclase, epidote, chlorite-penninite, allanite, and opaque minerals were frequently observed.

Plagioclase (2 to 24%) occurs as anhedral interstitial grains and as subhedral to euhedral inclusions within K-feldspar. Although not common, zoned plagioclase grains were observed and, as in other rock types, the cores of the zoned grains were more altered than outer portions. Alteration to kaolinite for all types of plagioclase ranged from minor to moderate. Inclusions of biotite, apatite, quartz, and allanite were frequently observed. Muscovite-sericite (0 to 10%) occurs as flakes of variable size both as interstitial grains and as inclusions within other minerals. Biotite (0 to 15%) also occurs as flakes of variable size and commonly has opaque minerals, allanite, apatite, chlorite, and muscovite associated with it. Zircon, apatite, sphene, tourmaline, epidote, allanite, fluorite, and chlorite-penninite occur in trace amounts disseminated throughout the samples and as inclusions within other mineral grains. Opaque minerals (tr to 5%) occur predominantly as subhedral to euhedral grains or inclusions and less frequently as anhedral masses.

HORNBLENDE ANDESITE PORPHYRIES

A total of five (5) samples were found to be hornblende andesite porphyries. The samples were found to consist of an aphanitic groundmass with phenocrysts or grains of quartz, plagioclase, hornblende, biotite, chlorite-penninite, epidote, sphene, calcite, zircon, and opaque minerals.

The groundmass (35 to 62%) of all five samples is aphantic and is extensively altered making positive identification of its components difficult. However, quartz, K-feldspar, and plagioclase laths were observed within the cryptofelsitic groundmass. Quartz (0 to 5%) occurs as anhedral phenocrysts possessing the somewhat straight sides, rounded corners, and aphanitic embayments characteristic of quartz of volcanic origin. Inclusions of hornblende were observed within some quartz phenocrysts. Quartz was also observed as a vesicle filling. Plagioclase (5 to 36%) occurs as subhedral to euhedral phenocrysts the majority of which are zoned. Alteration to kaolinite is quite abundant, ranging from moderate to extensive. Occasional embayments or blebs of groundmass were observed within the plagioclase phenocrysts. Most plagioclase phenocrysts also have corroded outlines suggesting reaction with the groundmass material. Hornblende (10 to 35%) occurs as subhedral to euhedral pseudohexagonal phenocrysts of varying size or thin rods. Both green and brown varieties of hornblende were observed. Iron oxide rims were frequently observed around hornblende phenocrysts. Minor propylitization due to hydrous deuteric solutions rich in CO_2 has caused some replacement of hornblende by chlorite-penninite, calcite, sphene, epidote, and iron oxides. Biotite (0 to 2%) occurs as subhedral phenocrysts which also show some effects of propylitization. Chlorite-penninite (1 to 9%) occurs as pseudomorphs after hornblende and commonly has epidote and calcite associated with it. In some instances, chlorite-penninite was observed as a vesicle filling along with epidote, calcite, and quartz. Epidote (0 to 3%) occurs primarily as a replacement mineral of hornblende. In some cases, almost complete replacement of hornblende by epidote is suspected. It also occurs as a vesicle filling along with chlorite-penninite, calcite, and quartz. Sphene, in addition to being a propylitization product of hornblende, also occurs in trace amounts as subhedral to euhedral phenocrysts displaying the typical acute rhombic section. Calcite (0 to 5%) occurs predominantly as a vesicle filling and to a lesser extent as a replacement of hornblende. As mentioned previously, it commonly is associated with chlorite-penninite and epidote. Zircon was observed as a trace mineral in two of the samples. Opaque minerals (2 to 4%) occur as anhedral to subhedral grains disseminated throughout the samples and occasionally as clusters.

ANDESITE PORPHYRIES

A total of thirty-one (31) samples were identified as andesite porphyries. They consist of aphanitic groundmass with phenocrysts or grains of plagioclase, K-feldspar, quartz, hornblende, biotite, chlorite-penninite, epidote, calcite, sphene, apatite, zircon, zeolites, and opaque minerals.

The groundmass (34 to 80%) of the andesite porphyries is similar to that of the hornblende andesite porphyries. It is aphanitic, extensively altered, and has a cryptofelsitic appearance. Quartz, plagioclase, and K-feldspar were occasionally identified within the groundmass. Plagioclase (6 to 50%) occurs as subhedral to euhedral phenocrysts, the majority of which are zoned. Alteration to kaolinite is extremely variable, ranging from virtually none to extensive. Occasional replacement by calcite was observed. The outlines of some plagioclase phenocrysts are corroded as the result of reaction with the groundmass. Inclusions of hornblende, chlorite-penninite, and quartz were observed. K-feldspar (0 to 5%), although not very common, occurs as subhedral to euhedral phenocrysts of sanidine which commonly have a corroded appearance. Inclusions of epidote, hornblende, and plagioclase were observed within K-feldspar phenocrysts. Quartz (0 to 7%) occurs as anhedral phenocrysts possessing the somewhat straight sides, rounded corners, and aphanitic embayments characteristic of quartz of volcanic origin. Occasional reaction rims with the groundmass were observed. Quartz also occurs as a vesicle filling in several samples. Inclusions of hornblende, biotite, and chlorite-penninite were observed. Hornblende (0 to 19%) occurs as subhedral to euhedral pseudohexagonal phenocrysts and thin rods of variable size. Both green and brown varieties were observed. Replacement-alteration due to propylitization is variable in extent ranging from minor to almost complete. The replacement-alteration minerals include chlorite-penninite, calcite, sphene, epidote, and iron oxides. Rims of iron oxides were frequently observed. Biotite (0 to 12%) occurs as flakes of varying size disseminated throughout the samples. Propylitization has caused much of the biotite to be replaced by chlorite-penninite and opaque minerals. Chlorite-penninite (2 to 20%), epidote (0 to 3%), and calcite (0 to 15%) occur predominantly as replacement minerals of hornblende and biotite. In addition to occurring as replacement minerals, chlorite-penninite, epidote, and calcite occur as vesicle fillings. Sphene (0 to 1%) occurs both as a replacement mineral for mafics and as distinct acute rhombic euhedral phenocrysts disseminated throughout the samples. Zircon and apatite occur in trace amounts predominantly as inclusions within other minerals. Zeolites (12%)

were observed only in sample 1012 where they occur as fibrous radial aggregates with nearly square cross section crystals also present. The zeolites occur as secondary minerals filling vesicles and as rims around feldspar phenocrysts. Opaque minerals (tr to 5%) occur as subhedral to euhedral grains disseminated throughout the samples, as rims on hornblende phenocrysts, and as a replacement of hornblende and biotite.

HORNBLENDE DIORITE PORPHYRY

Sample 1021 was found to be a hornblende diorite porphyry consisting of groundmass, plagioclase, hornblende, chlorite-penninite, sphene, and opaque minerals.

The groundmass (46%) is an allotriomorphic-granular mixture of plagioclase with lesser amounts of quartz and K-feldspar. Plagioclase (20%) occurs as subhedral to euhedral phenocrysts, the majority of which are zoned. Minor to moderate amounts of alteration were shown by plagioclase. Hornblende (25%) occurs as subhedral to euhedral phenocrysts of varying size. Minor to moderate replacement of hornblende by chlorite-penninite was observed. Chlorite-penninite (7%) occurs as a replacement mineral of hornblende. Sphene occurs in trace amounts as acute rhombic grains disseminated throughout the sample. Opaque minerals (1%) occur as euhedral to subhedral grains disseminated throughout the sample.

DIORITE PORPHYRIES

A total of five (5) samples were found to be diorite porphyries. The samples consist of groundmass with phenocrysts or grains of plagioclase, quartz, hornblende, biotite, chlorite-penninite, calcite, epidote, sphene, apatite, zircon, zeolites, and opaque minerals.

The groundmass (40 to 54%) is phaneritic in size and allotriomorphic-hypidiomorphic in texture. It is composed predominantly of plagioclase with lesser amounts of K-feldspar and quartz. The groundmass shows minor to moderate alteration of its components. Plagioclase (25 to 35%) occurs as subhedral to euhedral phenocrysts, most of which are zoned. Minor to moderate alteration to kaolinite was observed. Some phenocrysts are rimmed by quartz and feldspar intergrowths. Quartz (0 to 5%) occurs as anhedral to subhedral phenocrysts displaying volcanic features. Hornblende (0 to 9%) occurs as subhedral to euhedral phenocrysts which show minor to extensive replacement by chlorite-penninite, epidote, and calcite. Twinned phenocrysts were commonly observed. Biotite (0 to 15%) occurs as subhedral phenocrysts of variable size, most of which show some replacement by chlorite-penninite. Chlorite-penninite (0 to 10%), calcite (0 to 8%), and epidote (0 to 5%) occur as replacement minerals of hornblende and biotite. Sphene occurs as trace acute rhombic grains disseminated throughout the samples. Apatite and zircon occur in trace amounts as inclusions within other mineral grains. Zeolites (2%) occur in sample 1007 as radial fibrous aggregates of secondary origin. Opaque minerals (1 to 5%) occur as subhedral grains disseminated throughout the samples and as replacement minerals of hornblende and biotite.

APPENDIX D (continued)

DACITE PORPHYRIES

A total of three (3) samples were identified as dacite porphyries consisting of groundmass with phenocrysts or grains of plagioclase, K-feldspar, quartz, hornblende, biotite, chlorite-penninite, epidote, calcite, sphene, and opaque minerals.

The groundmass (39 to 49%) of the dacite porphyries is aphanitic and appears to consist predominantly of feldspar and quartz. Minor amounts of alteration of the groundmass were observed. Plagioclase (20 to 35%) occurs as subhedral to euhedral, predominantly zoned phenocrysts which display minor alteration to kaolinite. Some replacement of plagioclase by calcite was observed. Inclusions of hornblende and chlorite-penninite are present in some plagioclase phenocrysts. Although not abundant, K-feldspar (0 to 6%) (sanidine) occurs as subhedral to euhedral phenocrysts which show minor alteration. Calcite replacement was observed in some phenocrysts. Some inclusions of plagioclase and hornblende are present. Quartz (12 to 15%) occurs as subhedral phenocrysts with somewhat straight sides, rounded corners, and embayments of aphanitic material. Hornblende was observed as an inclusion in quartz phenocrysts. Hornblende (tr to 8%) occurs as subhedral to euhedral phenocrysts which show varying amounts of replacement by chlorite-penninite, epidote, and calcite. Biotite occurs as trace subhedral flakes of varying size the majority of which show replacement by chlorite-penninite, epidote, and calcite. Chlorite-penninite (5 to 10%), epidote (tr to 3%), and calcite (0 to 3%) occur as replacement minerals of hornblende and biotite. Sphene occurs as trace acute rhombic grains disseminated throughout the samples. Opaque minerals occur as trace subhedral to euhedral grains disseminated throughout the samples and occasionally associated with chlorite-penninite.

QUARTZ LATITE PROPHYRIES

A total of three (3) samples were found to be quartz latite porphyries consisting of groundmass with phenocrysts or grains of plagioclase, K-feldspar, quartz, biotite, hornblende, chlorite-penninite, epidote, calcite, sphene, apatite, allanite, and opaque minerals.

The groundmass (26 to 61%) is aphanitic and appears to be composed of quartz and feldspar. The groundmass shows signs of minor to moderate alteration. Plagioclase (10 to 25%) occurs as subhedral to euhedral phenocrysts, most of which show minor to moderate alteration to kaolinite. Inclusions of hornblende, epidote, and chlorite-penninite were frequently observed. K-feldspar (10 to 15%) (sanidine, orthoclase) occurs as subhedral to euhedral phenocrysts which show minor alteration to kaolinite-sericite. Some sanidine appears to be corroded. Inclusions of plagioclase were observed. Quartz (10 to 15%) occurs as subhedral phenocrysts with somewhat straight sides, rounded corners, and embayments of aphanitic material. Inclusions of hornblende and chlorite-penninite are present in some quartz phenocrysts. Hornblende (tr) and biotite (0 to 2%) occur as subhedral to euhedral phenocrysts which commonly show replacement by chlorite-penninite, calcite, and epidote. In addition to occurring as a replacement of hornblende and biotite, chlorite-penninite (tr to 6%), calcite (tr), and epidote (0 to tr) also occur as vesicle fillings. Sphene, apatite, and allanite occur in trace amounts both disseminated throughout the samples and as inclusions within other mineral grains. Opaque minerals (tr to 1%) occur as subhedral to euhedral grains disseminated throughout the samples.

HORNBLENDE ANDESITES

A total of four (4) samples were identified as hornblende andesites. The samples were found to consist of plagioclase, quartz, hornblende, chlorite-penninite, epidote, apatite, and opaque minerals. All four samples are fine grained with their minerals of similar sizes so that the term "groundmass" cannot be used.

Plagioclase (34 to 48%) occurs as small subhedral to euhedral laths and grains, the majority of which show signs of moderate alteration. Quartz (1 to 5%) occurs predominantly as secondary vesicle fillings and to a lesser extent as anhedral to subhedral grains. Hornblende (28 to 50%) occurs as subhedral to euhedral pseudohexagonal grains and as long thin rods. Replacement by chlorite-penninite (8 to 25%) and epidote (0 to 1%) was quite common. Chlorite-penninite also occurs as secondary vesicle fillings. Apatite occurs in trace amounts as inclusions within other minerals. Opaque minerals (tr to 4%) occur as anhedral to subhedral grains disseminated throughout the samples.

ANDESITE

Sample 1090-1 was identified as an andesite and was found to consist of plagioclase, quartz, biotite, chlorite-penninite, calcite, zircon, apatite, and opaque materials.

Plagioclase (57%) occurs as subhedral to euhedral grains which are moderately to extensively altered. Quartz (6%) occurs both as a secondary vesicle filling and as anhedral grains. Biotite (5%) occurs as subhedral flakes which show extensive replacement by chlorite-penninite and calcite. Chlorite-penninite (15%) also occurs as a replacement of unknown mafic minerals and occasionally as a secondary vesicle filling with calcite (8%). Zircon and apatite were observed as trace inclusions within other mineral grains. Opaque minerals (7%) occur as anhedral to subhedral grains disseminated throughout the sample.

AMPHIBOLITE XENOLITHS

Sample 1041, a xenolith, was found to be an amphibolite consisting of quartz, plagioclase, hornblende, pyroxene, chlorite-penninite, epidote, zircon, and opaque minerals.

Quartz (30%) and plagioclase (13%) occur both in segregation layers and in other portions of the sample where they are commonly poikilitically enclosed by hornblende. Plagioclase shows minor alteration to kaolinite.

Hornblende (32%) occurs as large predominantly blue-green poikilitic grains. Pyroxene (8%) (diopside) occurs as small anhedral to subhedral grains in somewhat segregated layers with quartz. Chlorite-penninite (10%) occurs disseminated throughout the sample and in one conspicuous layer with opaque minerals and quartz. Epidote (2%) occurs as disseminated grains throughout the sample. Trace amounts of zircon are disseminated throughout the sample. Opaque minerals (3%) occur both in disseminated form and in abundance in a zone with chlorite-penninite.

Sample 1051, a xenolith, was also identified as an amphibolite, but differs mineralogically from sample 1041. Sample 1051 consists only of quartz, plagioclase, hornblende, epidote, and opaque minerals.

Quartz (20%) and plagioclase (20%) occur in segregated layers as large grains and as smaller grains which are poikilitically enclosed by hornblende. Hornblende (56%) occurs as large poikilitic grains and as clusters of smaller grains. Epidote (3%) occurs as disseminated grains and as thin veins which frequently cut other minerals. Opaque minerals (1%) occur in disseminated form throughout the sample.